

THE ABSOLUTE MAGNITUDES OF RR LYRAE STARS AND THE AGE OF THE GALACTIC GLOBULAR CLUSTER SYSTEM

ALLAN SANDAGE¹

The Observatories of the Carnegie Institution of Washington

AND

CARLA CACCIARI

Osservatorio Astronomico di Bologna and Space Telescope Science Institute

Received 1989 April 24; accepted 1989 August 17

ABSTRACT

Various calibrations of the absolute magnitudes of RR Lyrae stars as a function of $[\text{Fe}/\text{H}]$ are reviewed and compared. The steep luminosity dependence on metallicity of $dM_V(\text{RR})/d[\text{Fe}/\text{H}] = 0.37$ previously derived from the periods, temperatures, and masses of RR Lyrae stars from the pulsation equation is the same as has recently been obtained by Buonanno, Corsi, and Fusi Pecci from main-sequence fitting of their faint-cluster photometry. In this paper we also find a similar slope for the RR luminosity-metallicity dependence using a new calibration of the position of the zero-age main sequence for stars of different metallicity. However, the very high sensitivity (and therefore relative uncertainty) of the slope determination to the positions of the zero-age main sequences for different $[\text{Fe}/\text{H}]$ values is shown.

Calibration of RR Lyrae luminosities determined from the period-shift data studied earlier, when combined with adopted precepts for RR Lyrae masses as a function of $[\text{Fe}/\text{H}]$, gives $M_V(\text{ZARR}) = 0.39[\text{Fe}/\text{H}] + 1.27$ for the zero-age horizontal-branch RR Lyrae stars, determined from the pulsation method. This slope dependence on metallicity is nearly the same as that determined from the main-sequence fits made by Buonanno, Corsi, and Fusi Pecci and from our own version of the main-sequence fitting method, but is more than a factor of 2 larger than $dM_V(\text{RR})/d[\text{Fe}/\text{H}] = 0.19$ found by combining several recent calibrations using the Baade-Wesselink method. At the moment it is not possible to decide between the various calibrations.

Ages of the halo clusters studied by Buonanno and coworkers have been determined from the absolute magnitudes of the main-sequence turnoff points found in various ways that use the several RR Lyrae $M_V(\text{RR})$ calibrations, and also directly from main-sequence fits independent of RR Lyrae star luminosities. With no $[\text{O}/\text{Fe}]$ enhancement as $[\text{Fe}/\text{H}]$ decreases, adopting $M_V(\text{ZARR}) = 0.39[\text{Fe}/\text{H}] + 1.27$ from the period-shift pulsation analysis gives a mean age for this cluster sample of 17 Gyr with virtually no dependence on metallicity. However, if there is an oxygen enhancement of $[\text{O}/\text{Fe}] = +0.6$ for $[\text{Fe}/\text{H}] < -1$, the mean age decreases by 23% to 14 Gyr, again nearly independent of $[\text{Fe}/\text{H}]$. On the other hand, if the slope dependence of $M_V(\text{RR})$ on $[\text{Fe}/\text{H}]$ is as small as 0.19, as given by the current data from the Baade-Wesselink method, then an age variation of the globular cluster system of $\sim 20\%$ would exist over the metallicity range for $[\text{Fe}/\text{H}]$ of -0.8 to -2.2 , the metal-rich clusters being younger.

Determination of the main-sequence turnoff luminosity directly from main-sequence fits gives an age for the globular cluster system of 19 Gyr for no oxygen enhancement, and 15.5 Gyr for a constant oxygen abundance enhancement of $[\text{O}/\text{Fe}] = +0.6$, again with no measurable dependence on metallicity. Each of these absolute age values is uncertain by 20% if the estimates of absolute luminosities, either of the RR Lyrae stars or of the main-sequence turnoff points, are uncertain by 0.2 mag.

Subject headings: clusters: globular — stars: abundances — stars: evolution — stars: RR Lyrae

I. INTRODUCTION

The only known reliable way to determine ages of star clusters in which all stars are coeval is to measure the main-sequence turnoff luminosity and to relate that evolutionary state to a Schönberg-Chandrasekhar (1942)-like change in the stellar structure (Sandage and Schwarzschild 1952; Schwarzschild 1958; Sandage 1958). But given even a perfect solution to the theory of the Schönberg-Chandrasekhar effect after nearly four decades of elegant model building by many astronomers, the observer's problem of measuring credible values of the turnoff luminosities still remains. In this regard, some soberness eventually dominates even the most optimistic hopes

when it is remembered that an error of only 0.1 mag in the turnoff luminosity produces a 10% error in the age.

Two methods are currently in use to measure the M_{bol} turnoff luminosities of globular clusters. (1) Direct main-sequence fitting of an observed color-magnitude ($C-M$) diagram to a grid of fiducial main sequences for different metallicities gives $M_V(\text{TO})$ directly. The chief disadvantage of this method is its high sensitivity to errors in the adopted reddening; the slope of the main sequence at the fitting points is $dM_V/d(B-V) = 7!$ In addition, any uncertainties in the positions of the fiducial main sequences for different $[\text{Fe}/\text{H}]$ values also enter directly as uncertainties in $M_V(\text{TO})$. (2) In principle, a more accurate method for finding $M_{\text{bol}}(\text{TO})$ is to measure the magnitude difference between the horizontal branch (in the RR Lyrae region) and the turnoff, to which is added an adopted

¹ Part of this work was completed while the first author was a Visiting Astronomer at The Johns Hopkins University and the Space Telescope Science Institute, Baltimore, Maryland.

value for the absolute magnitude of the RR Lyrae stars at any given cluster metallicity (Sandage 1982, hereafter S82). The method is very powerful because it is independent of reddening and of the position of the fiducial main sequence for different metallicities. Its accuracy does depend, of course, on the accuracy of the RR Lyrae luminosities for different metallicities. This calibration is imprecisely known at present, probably at the level of ~ 0.2 mag (cf. Sandage 1990*b*, hereafter S90*b*; and later in this paper).

This second method via the RR Lyrae stars can be used in two forms. (1) The $\Delta V(\text{TO} - \text{ZAHB})$ magnitude difference for each cluster individually can be used to determine $M_V(\text{TO})$ directly, once some particular $M_V(\text{RR}) = f([\text{Fe}/\text{H}])$ calibration is adopted, or (2) a mean value of $\Delta V(\text{TO} - \text{ZAHB}) = 3.54$ (say; see later) can be adopted for the cluster system as a more reliable value than the $\Delta V(\text{TO} - \text{ZAHB})$ value for any individual cluster. In this paper we shall use each of these three methods to determine $M_{\text{bol}}(\text{TO})$ and hence the ages for the 18 clusters studied by Buonanno, Corsi, and Fusi Pecci (1988, hereafter BCF) in their new CCD main-sequence photometry.

In the next section we use the BCF normal points for their 18 clusters and fit them to a grid of adopted fiducial main sequences for different $[\text{Fe}/\text{H}]$ values. The zero point of this grid has been defined using trigonometric parallax stars of high weight that have solar metal abundance. The main-sequence positions for other abundances are adopted from the Vandenberg and Bell (1985, hereafter VB) isochrones. A parallel fitting of the same BCF data to the zero-age main-sequence positions of the new Yale isochrone calibrations (Green, Demarque, and King 1987) is made in the Appendix.

In the second part of the next section we use the cluster distances obtained from this main-sequence fitting procedure to obtain $M_V(\text{RR})$ for the RR Lyrae stars (reduced to the zero-age horizontal branch [ZAHB]) in each cluster.

In § III the resulting $M_V(\text{RR}) = f([\text{Fe}/\text{H}])$ calibration from the MS fittings is compared with the $M_V(\text{RR})$ calibration obtained earlier by combining pulsation theory with the observed period shifts (S82; S90*b*). In § IV a comparison is made of these $M_V(\text{RR})$ values with an independent calibration that has been obtained by several astronomers using the Baade-Wesselink method to determine $M_V(\text{RR})$. A summary comparison of eight different $M_V(\text{RR})$ calibrations using five different methods is made in § V.

Ages of the clusters, based on these $M_V(\text{RR})$ values as used with the individual $\Delta V(\text{TO} - \text{ZAHB})$ values and also with an adopted mean of $\langle \Delta V(\text{TO} - \text{ZAHB}) \rangle = 3.54$ mag for the cluster system, are set out in § VI, assuming no $[\text{O}/\text{H}]$ enhancement as $[\text{Fe}/\text{H}]$ decreases. The same calculations, but with $[\text{O}/\text{Fe}]$ enhancement, are made in § VII.

Finally, we show in § VIII the determination of ages by the method of main-sequence fitting in which $M_{\text{bol}}(\text{TO})$ is determined directly, making no use at all of the RR Lyrae absolute magnitudes.

II. CALIBRATION OF THE $M_V(\text{RR}) = f([\text{Fe}/\text{H}])$ RELATION USING MAIN-SEQUENCE FITS

A very steep dependence of $M_V(\text{RR})$ on metallicity, with a slope of $dM_V(\text{RR})/d[\text{Fe}/\text{H}] = 0.39$, was derived in an earlier paper (S90*b*, eq. [5] with eqs. [17] and [19] to give eq. [22] there) using period-shift data together with the double-mode RR Lyrae masses as a function of $[\text{Fe}/\text{H}]$. A strong depen-

dence was also found by BCF, using the direct method of main-sequence fitting, to be

$$M_V(\text{ZAHB}) = 0.37[\text{Fe}/\text{H}] + 1.29, \quad (1)$$

which has a slope similar to that found originally (S82) from the period-shift argument. (Note that eq. [1] refers to the ZAHB because of the method used by BCF in its derivation. They used the apparent magnitudes of the ZAHB rather than the mean of the RR Lyrae magnitudes in their data tables. We shall maintain the distinction between $M_V(\langle \text{RR} \rangle)$ and $M_V(\text{ZAHB})$ throughout this paper. A short discussion is in the final paragraph of this section.)

A considerably smaller slope of $dM_V(\text{RR})/d[\text{Fe}/\text{H}] = 0.19$ can also be obtained from the period-shift data for the variable stars if we arbitrarily assume that the RR Lyrae star mass is independent of $[\text{Fe}/\text{H}]$ (S90*b*, eq. [21]). Remarkably, this is also the slope obtained by combining the results of four independent investigations of many RR Lyrae stars using the Baade-Wesselink (BW) method, summarized in the next section.

Because of the difference in slopes obtained by these three independent methods of (1) the main-sequence fitting, (2) the pulsation data combined with the presently computed double-mode RR masses, and (3) the BW physical method, we consider more closely in this section the main-sequence fitting method. The purpose here is to evaluate the sensitivity of the $M_V(\text{RR})$ calibration using this method to small changes in the assumed position of the fiducial main sequences.

a) Position of the Fiducial Main Sequence for $[\text{Fe}/\text{H}] = 0$

The value of the Hyades distance is not required to define the position of the zero-age main sequence (ZAMS) for solar-abundance stars. There are enough unevolved stars of solar abundance with sufficiently large trigonometric parallaxes to define the ZAMS with an error for the position of the ridgeline of less than 0.02 mag without recourse to the Hyades distance. Figure 1 shows 34 such stars using data from the first Yale Catalog of Trigonometric Parallaxes (Jenkins 1952). Each plotted star has a listed percentage parallax error of less than 7% (1 σ values), which translates into a magnitude error of less than 0.15 mag (per star).

The drawn line in Figure 1 is the ZAMS adopted earlier (Sandage and Eggen 1959, Table III). Although this calibration was initially based on the Hyades main sequence as to shape and zero point (using the value of the Hyades modulus that was current at the time, before the revisions suggested by Hodge and Wallerstein 1966 and Wallerstein and Hodge 1967 were known), it nevertheless fits the trigonometric data well and therefore can be defined by them alone. Remarkably, the position of this line is nearly identical to the interpolation equation derived by Vandenberg and Poll (1989), based on the slope of the observed Pleiades main sequence and zero-pointed at $M_V = 4.989$ at $B - V = 0.64$ for reasons connected with theoretical main-sequence models with $[\text{Fe}/\text{H}] = 0$ as discussed by them.

Vandenberg and Poll's (1989) main-sequence equation, which, simply by coincidence, reproduces the drawn line in Figure 1 to within 0.01 mag, is

$$M_V = 2.836 - 6.796(B - V) + 31.77(B - V)^2 - 31.6(B - V)^3 + 10.57(B - V)^4. \quad (2)$$

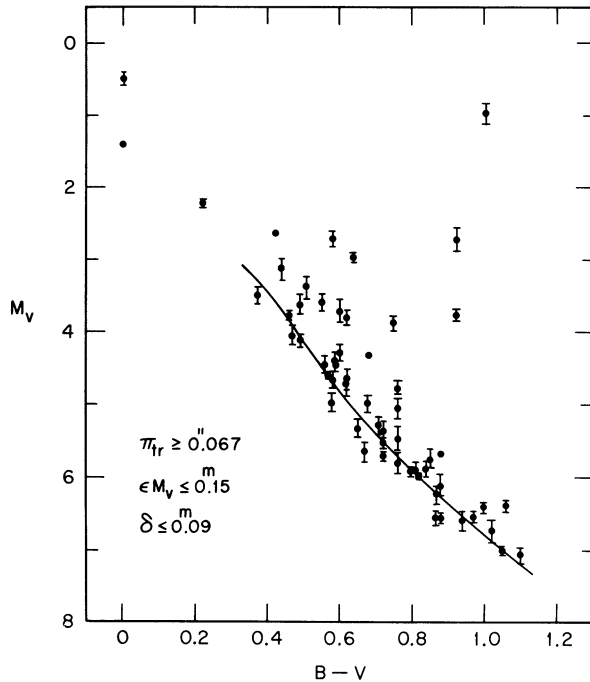


FIG. 1.—Color-magnitude diagram defined by trigonometric parallax stars of high weight that have solar metal abundance (in the mean). The drawn line is from Table III of Sandage and Eggen (1959). It is represented to within 0.01 mag by eq. (2) due to Vandenberg and Poll (1989).

b) Positions of the Zero-Age Main Sequences for Different Metallicities

Various calibrations exist of how the main sequence becomes fainter as the metal abundance decreases. Two effects must be considered, each with a different dependence on either the total metal abundance $[M/H]$ or only on the iron $[Fe/H]$ abundance. The $[M/H]$ value determines the main-sequence position in the $(\log T_e, M_{\text{bol}})$ -plane because this position depends on the internal opacity. On the other hand, the $[Fe/H]$ value determines the blanketing effect on the colors for the $C-M$ diagram. The iron abundance itself has little to do with the total opacity per se, because this is determined principally by the oxygen and neon abundances, which are about 250 times larger than the abundance of iron. But, if O varies in lockstep with Fe, then $[Fe/H]$ does measure that part of the opacity (to within a normalization factor) that is determined by bound-free transitions of the metals. (Note, however, that for $[M/H]$ smaller than -1 , the opacity is dominated by free-free transitions of H and He which are independent of $[M/H]$; cf. the comments later in this section.) However, if O does not track Fe, the $[Fe/H]$ value determines only the blanketing part of the effect, which is dominant in $B-V$ but not in the temperature T_e or the $R-I$ color. This will become an important point in the later discussion.

Ideally, the main-sequence depression in the $C-M$ diagram for decreasing $[Fe/H]$ values could be determined empirically from trigonometric parallax stars which have the appropriate $[Fe/H]$ values. This approach was followed in earlier determinations of the effect (Sandage and Eggen 1959; Eggen and Sandage 1962; Sandage 1970; Cameron 1985; van Alena *et al.* 1988). However, the available trigonometric parallax values are too poorly known to make a definitive determination in

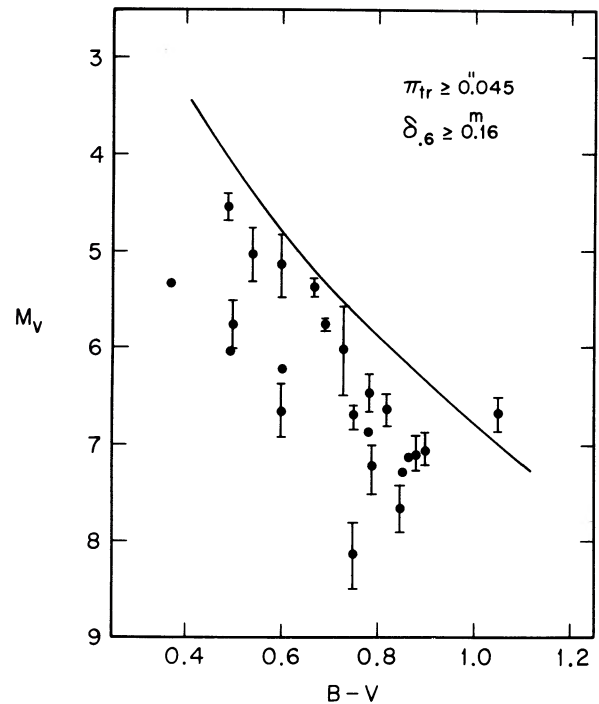


FIG. 2.—Trigonometric parallax stars with listed parallaxes larger than $0''.045$ that have UV excess values larger than 0.16 mag, corresponding to $[Fe/H] < -1$. The line is the same as that shown in Fig. 1 for the zero-age main sequence for $[Fe/H] = 0$.

this way, as shown in Figure 2. Plotted is the $C-M$ diagram for stars which have parallax values greater than $0''.045$ (regardless of the listed accuracy of the parallax) and that also have UV excess values larger than 0.16 mag. This excess translates to $[Fe/H]$ values smaller than -1 (e.g., Cameron 1985 for a calibration, following Wallerstein and Carlson 1960). Figure 2 shows the clear depression of the M_V values below the fiducial

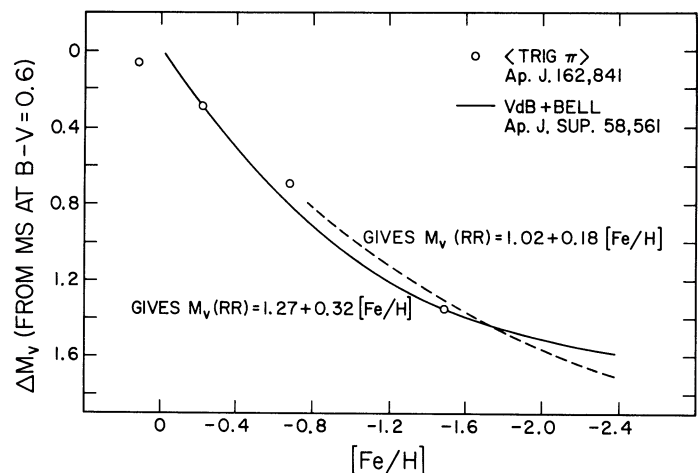


FIG. 3.—Adopted depression of the ZAMS below the fiducial sequence in Fig. 1 for different metallicities at fixed helium abundance. The solid line is from the theory calculated by Vandenberg and Bridges (1984) and by Vandenberg and Bell (1985). The four open circles are the mean of the trigonometric parallax stars used by Eggen and Sandage (1962) and by Sandage (1970). The dashed line is the relation that is required to produce an early, very slightly different, version of eq. (9) of the text for the Baade-Wesselink RR Lyrae calibration.

[Fe/H] = 0 sequence, but its size for any given [Fe/H] value is not well determined. We have, therefore, relied primarily on calculated models to calibrate the effect.

Figure 3 shows the correction function we have adopted. The solid line has been read at $B-V = 0.60$ from the theoretical $C-M$ diagram ZAMS models of Vandenberg and Bell (1985, Fig. 4) for [Fe/H] values between -0.49 and -2.27 , interpolating in their tables to $Y = 0.25$. For higher metal abundances, Figure 3 of Vandenberg and Bridges (1984) was used, also read at $B-V = 0.60$. These offsets were then zero-pointed to give a magnitude depression of zero at [Fe/H] = 0. Vandenberg and Poll's (1989) analytical interpolation equation for this magnitude depression, said by them to be valid only to [Fe/H] > -1.4 , is

$$dM_V = 2.6(Y - 0.27) - [\text{Fe}/\text{H}](1.444 + 0.362[\text{Fe}/\text{H}]), \quad (3)$$

which is, in fact, the solid line that is drawn for [Fe/H] > -1.6 , assuming $dM_V = 0$ at [Fe/H] = 0 and keeping Y constant as [Fe/H] is varied. (Alternatively, see the discussion in the Appendix, where it is argued that Y might be expected to vary with [Fe/H] as a way to adjust certain discrepancies discussed later in § V.) The agreement between equation (3) and the solid line in Figure 3 becomes poor for [Fe/H] < -1.6 because of the unphysical minimum in equation (3) at [Fe/H] = -2.0 . The line we have adopted in Figure 3 for [Fe/H] < -1.4 is from the VB models (Tables 5–13 interpolated to $Y = 0.25$), read at $B-V = 0.60$, which has the magnitude depressions and [Fe/H] values of 1.31 at -1.4 , 1.40 at -1.6 , 1.46 at -1.8 , 1.51 at -2.0 , 1.54 at -2.2 , and 1.58 at -2.4 . We have neglected the change of shape of this line with $B-V$ that can be seen by reading the VB curves at $B-V = 0.7$ and 0.8 . Since most of our main-sequence fittings are centered near $B-V = 0.6$, the error introduced by this approximation is small. Later in this section we show that if we had, in fact, used the change of shape of Figure 3 with $B-V$ (i.e., used nonparallel rather than parallel displacements for the family of main-sequence positions below the [Fe/H] fiducial sequence as a function of $B-V$), our final slope $dM(\text{RR})/d[\text{Fe}/\text{H}]$ would have been even steeper [cf. Fig. 3 for the effect of the change of shape of the line on the slope of $M_V(\text{RR})$ upon metallicity]. And we have taken into account the change of shape of the main sequences as [Fe/H] decreases in the analysis of the data using the Yale isochrones in the discussion in the Appendix, which also gives a steep slope to the $M_V(\text{RR})$ –[Fe/H] relation (see also the final comment in the final paragraph of this section).

The four open circles in Figure 3 are the values adopted earlier (Sandage 1970, Table 11) from averages of the moderately high weight trigonometric parallaxes for stars of the appropriate metallicity, with no Lutz-Kelker (1973) type corrections applied. The dashed line, explained more fully in § IV, is the required correction if the main-sequence fitting were to give the more shallow slope of $dM_V(\text{RR})/d[\text{Fe}/\text{H}] = 0.18$ for the RR Lyrae luminosity dependence. The difference between the solid and the dashed lines is minute, showing the high sensitivity of this most fundamental of the methods to magnitude differences as small as ~ 0.2 mag in the calibration.

The size of the magnitude depression reaches ~ 1.5 mag at [Fe/H] = -2.5 . Almost all of the effect for iron abundances smaller than [Fe/H] ~ -1 is due to blanketing, not to changes in the stellar interior model. This is because the bound-free opacity due to the metals falls below the free-free opacity of H and He for [M/H] < -1 , hence the total opacity does not

continue to decrease as [M/H] is decreased below this value. Therefore, the positions of the main sequences in the (M_{bol} , $\log T_e$)-diagram become insensitive to changes in [M/H] below [Fe/H] ~ -1 .

But this is not the case in the (M_V , $B-V$)-diagram, where blanketing by Fraunhofer lines (primarily iron) continue to affect the $B-V$ colors for smaller metal abundances. This point can be seen from the large difference between Figure 3 for the effect in $B-V$ and the equivalent diagram for the dM_V depression in $R-I$ given by Eggen (1987, Fig. 2), or in the tables given by VB and by Green, Demarque, and King (1987), where the dM_V correction changes very little for [Fe/H] < -1 in $R-I$. Therefore, Figure 3 is valid, in fact, for the true [Fe/H] iron abundances rather than for the true total metal [M/H] values. The iron lines cause the bulk of the UV blocking and therefore cause the UV excess from which [Fe/H] is determined. The point is that Figure 3 gives the appropriate correction to be made to the fiducial [Fe/H] = 0 main sequence in, for example, Figure 1 for any given [Fe/H] value regardless of any [O/Fe] enhancement. Calculated models by Vandenberg (1987, private communication) and by P. Demarque (1988, private communication) confirm this conclusion.

Figure 4 shows the result of combining Figure 1 (eq. [2]) for the fiducial main sequence at [Fe/H] = 0 (the drawn line) with the composition adjustment of Figure 3 to give the adopted ZAMS positions for the metallicities that are marked in the diagram. The dashed lines in Figure 4 have the same meaning as in Figure 3.

As we said above, the correction function in Figure 3 has been determined from ZAMS models at $B-V = 0.6$. But we have estimated the magnitude depression corrections at $B-V = 0.7$ and 0.8 as well. These corrections are systematically smaller by about 0.1 mag at $B-V = 0.7$ for [Fe/H] > -2 , but do converge to the $B-V$ values for [Fe/H] > -1.4 . This variation of Figure 3 with $B-V$ at the low

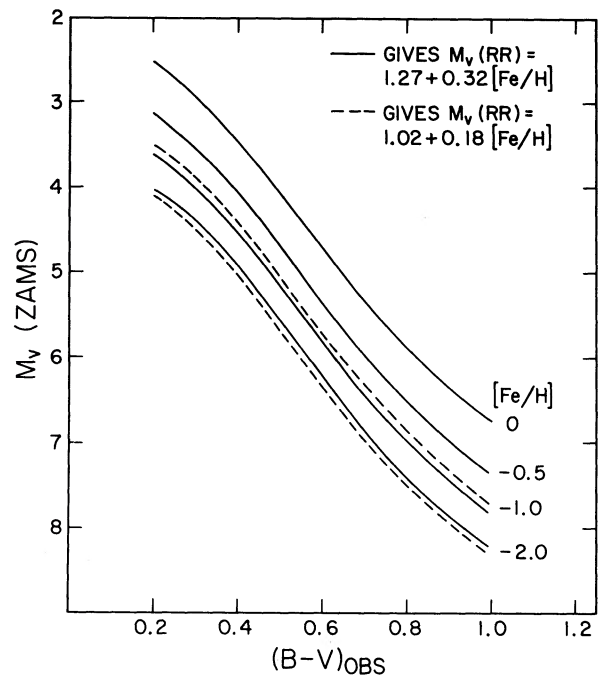


FIG. 4.—Adopted main-sequence positions in the color-magnitude diagram for different metallicities, obtained by combining Figs. 1 and 3.

TABLE 1
RR LYRAE AND MAIN-SEQUENCE TURNOFF LUMINOSITIES OBTAINED DIRECTLY FROM MAIN-SEQUENCE FITTING

Cluster (1)	[Fe/H] (2)	$E(B-V)$ (3)	$(m-M)_0^a$ (4)	V_o (HB) (5)	M_V (RR) (6)	V_o (TO) (7)	M_V (TO) (8)	$(B-V)_{TO}$ (9)	B.C. (10)	M_{bol} (TO) (11)	Age (12)
N104	-0.71	0.04	13.05	13.97±0.15	0.92±0.15	17.62	4.57	0.52	-0.09	4.48	18.3
N288	-1.40	0.04	14.41	15.27±0.10	0.86±0.10	18.82	4.41	0.44	-0.11	4.30	19.6
N362	-1.27	0.06	14.26	15.24±0.10	0.98±0.10	18.66	4.40	0.45	-0.09	4.31	18.9
N2808	-1.37	0.22	14.54	15.40±0.10	0.86±0.10	18.90	4.36	0.44	-0.11	4.25	18.5
N4590	-2.09	0.07	14.94	15.49±0.07	0.55±0.07	18.88	3.94	0.35	-0.11	3.83	16.0
N5139	-1.59	0.11	13.42	14.17±0.10	0.75±0.10	17.85	4.43	0.45	-0.12	4.31	21.1
N5272	-1.66	0.01	14.81	15.62±0.05	0.81±0.05	19.07	4.26	0.41	-0.11	4.15	18.6
N5904	-1.13	0.03	14.11	15.01±0.05	0.90±0.05	18.50	4.39	0.45	-0.10	4.29	17.7
N6121	-1.28	0.37	11.24	12.17±0.07	0.93±0.07	15.72	4.48	0.44	-0.10	4.38	20.3
N6171	-0.85	0.31	13.51	14.71±0.10	1.20	18.36	4.85	0.50	-0.09	4.76	(25.0)
N6205	-1.65	0.02	13.97	14.89±0.15	0.92±0.15	18.44	4.47	0.41	-0.11	4.36	22.6
N6341	-2.24	0.02	14.30	14.99±0.07	0.69±0.07	18.64	4.34	0.40	-0.12	4.22	24.3
N6397	-1.91	0.18	11.86	12.42±0.10	0.56±0.10	15.97	4.11	0.37	-0.12	3.99	17.4
N6752	-1.54	0.04	12.87	13.62±0.15	0.75±0.15	17.27	4.40	0.41	-0.11	4.29	20.4
N6809	-1.82	0.14	13.33	13.90±0.07	0.57±0.07	17.45	4.12	0.40	-0.11	4.01	17.2
N7078	-2.15	0.10	14.95	15.54±0.05	0.59±0.05	18.98	4.03	0.36	-0.12	3.91	17.6
N7099	-2.13	0.04	14.59	15.07±0.10	0.48±0.10	18.69	4.10	0.34	-0.11	3.99	18.8
Pal 5	-1.27	0.03	16.46	17.30±0.10	0.84±0.10	20.75	4.29	0.43	-0.10	4.19	16.9
											19.07±2.1(σ)

^a The col. (4) values are determined by main-sequence photometric fits to appropriate fiducial ZAMS positions for different [Fe/H] values.

metallicities is almost exactly compensated for by our neglect of the slight evolution of the actual globular cluster main-sequence position brightward from the ZAMS at $B-V = 0.6$ relative to $B-V = 0.7-0.8$, canceling the effect of nonparallel displacement of the fiducial main sequences as a function of $B-V$ as [Fe/H] decreases, as discussed more completely near the end of § IIc.

c) M_V (RR) Absolute Magnitude Values from Main-Sequence Fitting

In an obvious way, the main-sequence photometric data for the program clusters of BCF, listed in their Table II, were fitted to the grid of ZAMS positions in Figure 4 using appropriate [Fe/H] values. Our detailed procedure was to derive the dM_V correction from Figure 3, assuming fixed Y , and then to apply this value as a correction to the distance modulus obtained by fitting the data to the [Fe/H] = 0 main sequence of equation (2), which is the line in Figure 1. The fitting was done using only the faintest parts of the observed cluster main sequences (usually from $B-V = 0.6-0.75$), read at a number of discrete points, and averaging the resulting $m-M$ values. The formal error in the resulting mean modulus values has been generally less than 0.1 mag (average deviation).

We have adopted the $E(B-V)$ reddening values from BCF (their Table VIII). Applying these reddenings to the observed main-sequence colors, and using $3.2E(B-V)$ as the correction to the observed magnitudes, gives the distance modulus of each cluster by the fitting procedure just described. The absolute magnitude of the zero-age horizontal branch at the RR Lyrae gap follows directly by applying this value for the modulus to the apparent magnitude of the ZAHB, corrected for reddening.

The results are shown in Table 1. The program clusters from BCF are listed in column (1). The adopted metallicities in column (2) and the reddenings in column (3) are also from this source (Tables III and VIII of BCF). The distance moduli in column (4) are from the main-sequence fitting to Figures 1 and 4.

Column (5) lists the apparent magnitude of the lower envelope (assumed to be the ZAHB) of the observed horizontal branch in each cluster (from Table IV of BCF as compiled from the literature), again corrected for reddening by $3.2E(B-V)$. The resulting absolute magnitudes M_V (RR) of the ZAHBs of the clusters, which we are seeking, are in column (6). (Cols. [7]–[12] concern the age-dating problem, to be discussed in § VIII.)

The correlation of the RR Lyrae M_V (RR) values in column (6) with [Fe/H] is shown in Figure 5. The “impartial” least-squares line (found here from Seares’s 1944 method of combining the two slopes of the solutions by exchanging the

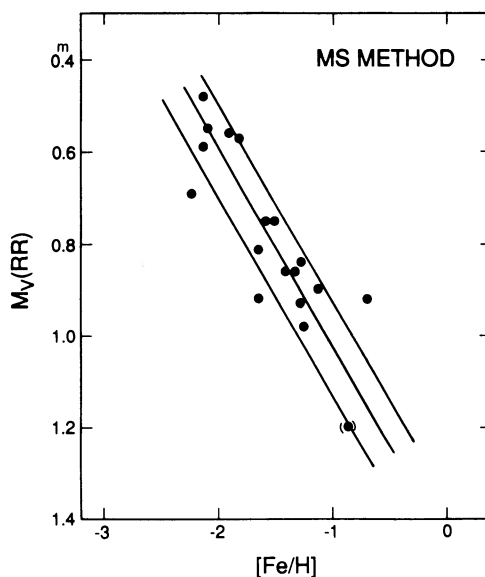


FIG. 5.—Correlation of the absolute magnitudes of RR Lyrae stars with metallicity obtained from main-sequence fits. The ridgeline is defined by eq. (4) of the text. The data are from cols. (2) and (6) of Table 1.

dependent and independent variables and adopting the mean slope to be the square root of the product of the two slopes, assuming equal errors in ordinate and abscissa), neglecting the uncertain point for NGC 6171, is

$$M_V(\text{RR}) = 0.38[\text{Fe}/\text{H}] + 1.39, \quad (4)$$

with the correlation coefficient of $r = 0.83$. The least-squares regression made by minimizing the residuals only in M_V at fixed $[\text{Fe}/\text{H}]$ is

$$M_V(\text{RR}) = 0.32[\text{Fe}/\text{H}] + 1.27. \quad (5)$$

Equations (4) and (5) agree well with the result of BCF from their independent main-sequence fits, given by equation (1) at the beginning of this section. This method, however, is extremely sensitive to the fitting procedure and to small changes in the theoretical and observed main sequences, especially for clusters at the metal-poor end of the metallicity range. As an example, we have repeated the fitting procedure using dM_V corrections read at $B-V = 0.7$ instead of 0.6, and we have obtained the corresponding expression to equation (5) as

$$M_V(\text{RR}) = 0.37[\text{Fe}/\text{H}] + 1.25. \quad (5a)$$

The small evolutionary effect that is present at $B-V = 0.6$ on the observed main sequences therefore has the effect of slightly decreasing the slope of this relation (i.e., eq. [5] compared with eq. [5a]), while the zero point is practically unaffected. The following analysis is not substantially modified by the use of equation (5) or equation (5a), but this exercise does show how very sensitive the results of this procedure are on even quite minor changes and assumptions (cf. the Appendix for one possible system of changes).

As discussed in the Appendix, this uncertainty can again be demonstrated by a comparison of our results with those of Green (1988), who found $M_V(\text{ZAHB}) = 0.20[\text{Fe}/\text{H}] + 0.84$ using the revised Yale isochrones (Green, Demarque, and King 1987). Green used different $C-M$ diagrams and a different fitting procedure that made compromise fits to a combination of the faint main sequence, the turnoff colors, and the shape of the red giant branch (RGB), in which, in fact, more weight was given to the turnoff and the RGB regions than to the faint main sequence. We have used only the faint main-sequence fit in our procedure.

Finally, it is to be emphasized that equations (4) and (5), because of their method of derivation via column (5) of Table 1, refer to the ZAHB. Taking into account the effects of measuring errors on the column (5) values of $V(\text{ZAHB})$ together with the average size of the post-ZAHB luminosity evolution, BCF estimate that $M_V(\text{RR})$ for a random sample of RR Lyrae stars will be ~ 0.1 mag brighter than the ZAHB values from equations (4) and (5). This is similar to the value estimated by one of us for the evolutionary mean HB brightening found from other considerations (S90a). We adopt the BCF estimate throughout the present paper.

III. COMPARISON WITH $M_V(\text{RR})$ FROM PULSATION THEORY

The calibration of RR Lyrae luminosities from the pulsation equation, using masses determined from the data on double-mode variables, gives (cf. S90b, by combining eqs. [5] and [19] there)

$$M_{\text{bol}}(\text{RR}) = 0.45[\text{Fe}/\text{H}] + 1.23. \quad (6)$$

The bolometric corrections for stars with the relevant surface gravities between $\log g$ of 3.0 and 3.5 and in the range of

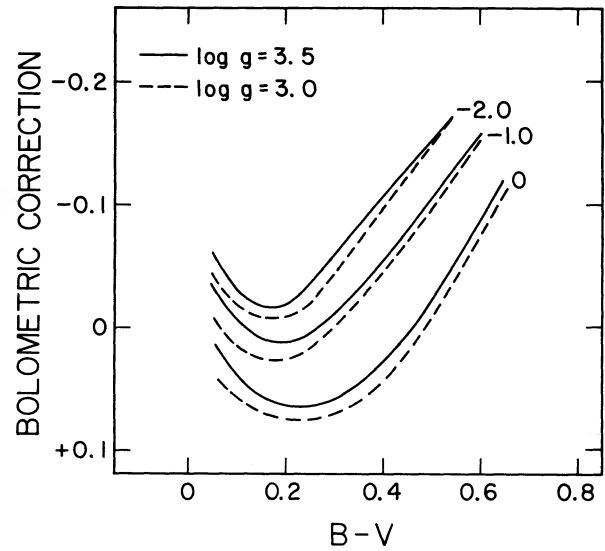


FIG. 6.—Adopted bolometric corrections for different $B-V$ colors for two different surface gravities and three different values of $[\text{Fe}/\text{H}]$.

temperatures covered by the RR Lyrae stars are shown in Figure 6. These are from tables kindly supplied by P. Demarque, Y.-W. Lee, and R. Zinn as used recently at Yale. The data are based on stellar models by R. L. Kurucz and others. Reading this diagram at the color equivalent to a temperature of $\log T_e = 3.85$ gives

$$\text{BC} = 0.06[\text{Fe}/\text{H}] + 0.06 \quad (7)$$

for the mean RR Lyrae bolometric correction (defined here with the sign convention of eq. [7] to be $M_V = M_{\text{bol}} - \text{BC}$). Combining this with equation (6) gives

$$M_V(\text{RR}) = 0.39[\text{Fe}/\text{H}] + 1.17 \quad (8)$$

for the calibration from the pulsation analysis. Equation (8) is equation (22) of S90b. From the method of derivation (the ridgeline rather than the lower envelope correlation of the $L/M^{0.81}$ ratio from Lub's 1987 eq. [5] set out in S90b), equation (8) refers to the mean of a random sample. As mentioned above, in § IV we shall take the ZAHB calibration to be 0.1 mag fainter than this ridgeline value.

It is worth emphasizing again (cf. S90b, § V, eq. [19]) that the slope in equation (8) is due to the adopted mass-metallicity relation for the variables obtained from the observations of double-mode pulsators combined with a theory for their period ratios as a function of mass. A shallower dependence of mass on metallicity, as suggested by the BW slope discussed in § IV (eq. [9]) or by the Lee, Demarque, and Zinn (1990, hereafter LDZ) theoretical models, would obviously produce a less steep slope in equation (8).

IV. $M_V(\text{RR})$ CALIBRATION USING THE BAADE-WESSELINK METHOD

Calibration of RR Lyrae absolute magnitudes using the Baade-Wesselink technique have been obtained recently for 25 variables by four research groups working independently.

A summary of the data by Cacciari *et al.* (1988), Cacciari, Clementini, and Buser (1988), Liu and Janes (1988), Jameson, Fernley, and Longmore (1987), and Jones, Carney, and Latham (1988) is set out in Table 2. The correlation of absolute

TABLE 2
ADOPTED M_V MAGNITUDES FOR FIELD RR LYRAE STARS
DETERMINED FROM THE BAADE-WESSELINK METHOD

Star (1)	M_V (2)	[Fe/H] (3)	Sources (4)
SW And	0.91	-0.15	1, 2
X Ari	0.63	-2.2	3, 4
RS Boo	0.95	-0.5	3
TV Boo	0.67	-2.15	2
YZ Cap	0.80	-1.3	5
RR Cet	0.80	-1.25	2
SU Dra	0.62	-1.75	2
SW Dra	0.82	-0.8	1, 3, 6
RX Eri	0.78	-1.32	2
SS For	0.73	-1.5	1
RR Gem	0.95	-0.29	2
TW Her	0.90	-0.5	3
RR Leo	0.81	-1.35	2
TT Lyn	0.74	-1.35	2
V455 Oph	1.02	-0.4	4
AV Peg	1.19	0.03	2
DH Peg	0.89	-0.8	3
AR Per	0.91	-0.60	2
RV Phe	0.77	-1.5	5
V440 Sgr	0.72	-1.4	5
T Sex	0.78	-1.20	2
VY Ser	0.77	-1.8	3, 4, 6
TU UMa	0.85	-1.3	2
UU Vir	0.82	-0.7	3
VV Vir	0.92	-0.49	2

REFERENCES.—(1) Cacciari *et al.* 1988; (2) Liu and Janes 1988; (3) Jones, Carney, and Latham 1988; (4) Jameson, Fernley, and Longmore 1987; (5) Cacciari, Clementini, and Buser 1988; (6) Buonanno, Corsi, and Fusi Pecci 1988.

magnitude with metallicity is shown in Figure 7, which has the least-squares regression found by minimizing the residuals in M_V alone, as

$$M_V(\text{RR}) = 0.19[\text{Fe}/\text{H}] + 1.03, \quad (9)$$

with the correlation coefficient of $r = 0.90$. Equation (9) refers to the calibration of a random sample. Again, in § VI, we assume that the ZAHB calibration is 0.1 mag fainter, consistent with the envelope lines in Figure 7 that are placed brightward and faintward by 0.1 mag from the ridgeline.

The smaller slope of 0.19 in equation (9) compared with ~ 0.4 obtained in the previous sections both from the pulsation and from the main-sequence calibrations has important consequences for the age determinations (§§ VI and VII). Therefore, it is of interest to determine the sensitivity of the results to the assumptions of each method. Consider first what must be done to the main-sequence positions to change the slope in equations (4) and (5) from approximately 0.4 to 0.2. By proceeding through the main-sequence fitting steps in reverse, we can determine, in an obvious way, how the calibrations in Figures 3 and 4 must be changed to produce any desired slope value. The dashed lines in these two diagrams show the result for the particular slope values shown. As mentioned earlier, the very high sensitivity of these slopes to small changes in the adopted calibration shows the relative uncertainty of the main-sequence fitting method. We would also have had some leeway in the result if we had chosen to vary Y with [Fe/H] in defining the positions of the various main sequences in Figure 4 (cf. the Appendix).

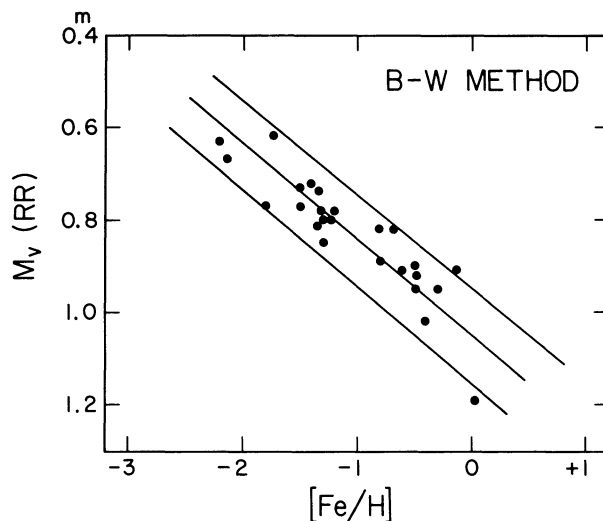


FIG. 7.—Summary of the absolute magnitude calibrations of RR Lyrae stars using the Baade-Wesselink method that have been obtained by four independent research groups. The data are reviewed in Table 2. The ridgeline is defined by eq. (9) of the text.

However the BW method, itself, is also at present uncertain in its fine details because it is much more complicated in principle (cf. Gautschy 1987) than the determinations using either the pulsation or the main-sequence method. Each of the four analyses that have gone into Figure 7, although independent, uses the same fundamental assumptions in the central methods of the computations. Each also uses the same current Kurucz model atmospheres, which, although the best that are available, are not yet definitive (R. L. Kurucz 1988, comment at the Van Vleck Observatory Age Dating Workshop). Hence, all of the BW results could be subject to a common systematic error, if such were later shown to exist.

Hence, because of uncertainties in (1) the main-sequence positions for different metallicities in the main-sequence fitting method, together with the remaining uncertainties in the various $C-M$ diagram photometries and in our fitting procedure, (2) masses in the pulsation period-shift method, and (3) perhaps model atmospheres in the BW method, we are left with uncertainties in the values for the $dM_V(\text{RR})/d[\text{Fe}/\text{H}]$ slopes. What appear to be equally defensible independent methods give slope values that range between ~ 0.2 and ~ 0.4 .

V. COMPARISON OF EIGHT $M_V(\text{RR})$ CALIBRATIONS

Four independent calibrations of the RR Lyrae absolute magnitudes as a function of metallicity are shown in Figure 8, based on equations (5), (8), and (9), reduced where necessary to the ZAHB level as explained earlier. The adopted ZAHB equations are set out within the borders of the diagram.

The horizontal line at $M_V = 0.80$, showing no dependence on metallicity, is the statistical parallax determination by Hawley *et al.* (1986), as slightly modified by Barnes and Hawley (1986), reduced to the ZAHB by making the literature value fainter by 0.1 mag.

The agreement between these four calibrations in the metallicity range from -1 to -2 is ~ 0.3 mag. At $[\text{Fe}/\text{H}] = -1.2$ they all agree, remarkably, to within 0.1 mag. Nevertheless, the difference in slope by a factor of 2 between the methods has a profound effect on the question of whether age spread

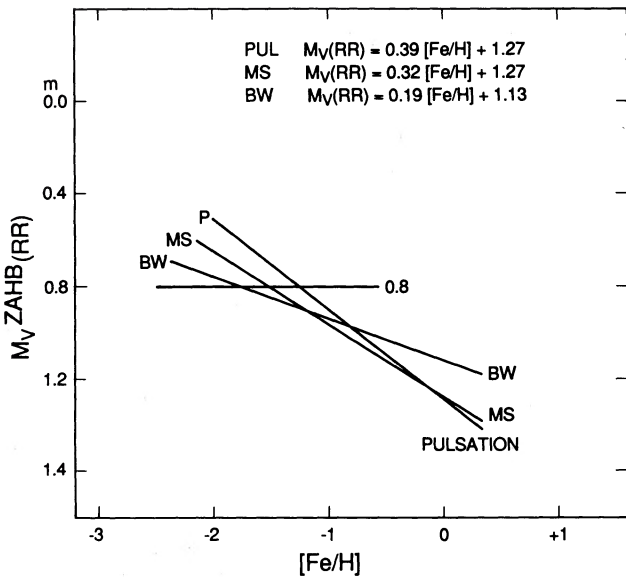


FIG. 8.—Summary of four calibrations of $M_V(\text{RR})$ for RR Lyrae stars for the ZAHB described in the text. The line marked BW is defined by eq. (9), to which 0.1 mag has been added to reduce the data to the ZAHB. The “pulsation” line from eq. (8) has also been changed to the ZAHB by adding 0.1 mag. The main-sequence line (MS) is from eq. (5).

depends on $[\text{Fe}/\text{H}]$, illustrating the extreme accuracy that is needed (apparently unattainable at present) for the $M(\text{RR}) = f([\text{Fe}/\text{H}])$ functions used in this method of solution for the age question (cf. § VI that follows).

A further comparison of other calibrations is shown in Figure 9. The data points are from the BW values in Table 2 and Figure 7. The line labeled $\langle \text{BCF} \rangle (\text{MS})$ is the main-sequence calibration of BCF given by equation (1). Considering its method of derivation, it refers to the ZAHB. The dashed line marked “Lub (field)” is from the calibration made by Lub (1987) from his Walraven photometry of field RR Lyrae stars of the $L/M^{0.81}$ ratio by assuming a constant value for the RR Lyrae masses. If, instead, a variable mass were to be used from

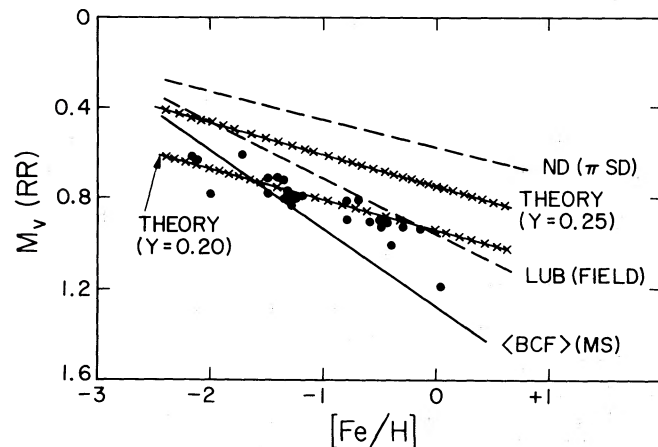


FIG. 9.—Summary of additional calibrations of the absolute magnitude of RR Lyrae stars as a function of metallicity. Details of the five illustrated lines are given in the text.

the mass-metallicity relation determined either from the double-mode variable star data or from the theory of the ZAHB (see Fig. 9a of S90b), the slope of Lub’s calibration, obtained by eliminating the mass from the observed $L/M^{0.81}$ ratio, becomes nearly the same as the line marked $\langle \text{BCF} \rangle$. The zero point of the calibration refers to a random sample, not the ZAHB.

The dashed line marked ND in Figure 9 is the main-sequence fit made by Noble and Dickens (1988) to a field subdwarf fiducial main-sequence position which they adopted from their rediscussion of the available trigonometric parallaxes. Their calibration of this fiducial main-sequence position is evidently about 0.6 mag brighter than shown in our analysis of the same problem in § II above, for reasons that are not known at this writing.

Finally, the two lines marked “theory” in Figure 9 are from the horizontal-branch models of Sweigart, Renzini, and Tornambè (1987, hereafter SRT) for two values of the helium abundance. From the H-R diagram in their Figure 1 we have read the luminosity of the ZAHB at the midpoint of the RR Lyrae strip (at $\log T_e = 3.85$) as a function of metallicity Z . From their Figure 1, the bolometric luminosity of the point on the ZAHB at $\log T_e = 3.85$ for three different Z -values is found for each of the three values of Y . By adopting the bolometric magnitude of the sun to be $M_{\text{bol}} = 4.75$, and by applying the bolometric correction (eq. [7] from Fig. 6) that is appropriate for the RR Lyrae stars, we find the SRT predicted calibrations to be

$$M_V(\text{RR}) = 0.15[\text{Fe}/\text{H}] + 0.95 \quad \text{for } Y = 0.20, \quad (10)$$

$$M_V(\text{RR}) = 0.13[\text{Fe}/\text{H}] + 0.74 \quad \text{for } Y = 0.25, \quad (11)$$

$$M_V(\text{RR}) = 0.10[\text{Fe}/\text{H}] + 0.54 \quad \text{for } Y = 0.30, \quad (12)$$

where the zero points are the theoretical values, arising from the assumptions made in deriving the ZAHB models. Because of inherent uncertainties in various input parameters in the theory, the zero points of equations (10)–(12) are probably less certain than the slope values, which only depend on differential variations. Equations (10) and (11) are shown as the cross-hatched lines in Figure 9.

In passing, we should note again that if the true calibration of the RR Lyrae star luminosities has as steep a metallicity dependence as $dM_V(\text{RR})/d[\text{Fe}/\text{H}] \sim 0.35$ that is given by some of the methods previously described, then, because these lines cut across the theoretical lines of constant helium abundance in Figure 9, one is forced to an anticorrelation of Y and Z to explain these $M_V(\text{RR})$ calibrations (shown in yet a different way in Figs. 10 and 11 of S90b). This, of course, is the same argument, only in a different form, that has been made by many authors based on the RR Lyrae period-shift problem (see, e.g., SRT, BCF, and S90b for reviews). One way out of this undesirable requirement is the solution by Lee, Demarque, and Zinn (1990), where no ZAHB RR Lyrae stars are said to exist in Oosterhoff type II clusters and, hence, where the ZAHB theory would not then apply in any interpretation of the period-shift data (cf. S90b). This solution implies, however, that a significant population of blue HB stars that have evolved off the ZAHB should exist in Oosterhoff type II clusters, against observational evidence in, say, M15 and NGC 5053. Furthermore, as discussed in some detail in S90b, the masses of the RR Lyrae stars that are predicted by the LDZ simulation disagree with the variation of mass with $[\text{Fe}/\text{H}]$ found for the double-

mode variables in the metal-poor cluster M15 and the more metal-rich clusters of M3 and IC 4499. These disagreements, for the moment, cloud the issue.

VI. CLUSTER AGES USING VARIOUS CALIBRATIONS OF RR LYRAE LUMINOSITIES AS FUNCTIONS OF METALLICITIES ASSUMING NO OXYGEN ENHANCEMENT

a) Procedure

The three types of data which must be known to calculate the age of any cluster are (1) the bolometric luminosity of the main-sequence turnoff point, (2) the helium abundance, and (3) the abundance of the metals that contribute to the interior opacity and to the energy generation. Item 3 is proportional to $[\text{Fe}/\text{H}]$ if all elements heavier than boron track with the iron abundance. If not, the relevant metal abundance depends on the absolute oxygen and neon abundances, which can be obtained from the Fe abundance once $[\text{O}/\text{Fe}]$ is known. As mentioned, O and Ne are the crucial elements for the opacity because they are about 250 times the Fe abundance.

Following the demonstration by Simoda and Iben (1968, 1970) and Iben and Rood (1970) that the age for a given turnoff luminosity depends on metallicity, major isochrone tables for various metallicities have been calculated by a number of workers. Widely used are the Yale tables of Ciardullo and Demarque (1977, hereafter CD), and more recently the tables by VandenBerg (1983) and by VB. An approximation to the Yale tables, derived elsewhere (Sandage, Katem, and Sandage 1981, eq. [18] and their Fig. 14), good to better than about 5% over the parameter range of interest, is

$$\log T(\text{yr}) = 8.319 + 0.41M_{\text{bol}}(\text{TO}) - 0.15[\text{Fe}/\text{H}] - 0.43(Y - 0.24). \quad (13)$$

Using the VB tables, Buonanno (1986, eq. [1]) finds

$$\log T(\text{yr}) = 8.49 + 0.37M_V(\text{TO}) - 0.13[\text{Fe}/\text{H}] \quad (14)$$

for $Y = 0.23$. Our own interpolation within these tables for $Y = 0.24$ gives

$$\log T(\text{yr}) = 8.394 + 0.39M_{\text{bol}}(\text{TO}) - 0.15[\text{Fe}/\text{H}]. \quad (15)$$

The agreement between these different versions of the dating equation is excellent in the slope dependences on M_{bol} and on $[\text{Fe}/\text{H}]$. Over the relevant parameter range of M_{bol} between 3.8 and 4.5 (see Fig. 15 below) and $[\text{Fe}/\text{H}]$ between -0.8 and -2.2 , one can find differences in the absolute age values of up to about 1 Gyr (less than 7%), with no indication, however, of a systematic offset between the equations. Because of the finer grid and the larger range in ages in the CD tables than in the VB listings, we adopt equation (13) in the remaining discussion, but note that the conclusions would be nearly identical had we used equation (14) or equation (15).

As discussed in § I, $M_{\text{bol}}(\text{TO})$ for the turnoff can be determined in three ways from the observations, two of which rely on the absolute magnitudes of the RR Lyrae stars.

A. The distance modulus of a given cluster is determined by subtracting some adopted value for the RR Lyrae absolute magnitudes from the observed apparent magnitude of the zero-age horizontal branch. The resulting distance modulus is then subtracted from the observed apparent magnitude of the main-sequence turnoff to give $M_V(\text{TO})$, to which the bolometric cor-

rection from some version of Figure 6 is applied to obtain $M_{\text{bol}}(\text{TO})$.

B. The absolute magnitude of the RR Lyrae stars is calculated from any one of the adopted calibrations we have been discussing. For each cluster, we add an adopted mean value of the difference in apparent magnitude between the ZAHB and the turnoff to this calculated absolute magnitude of the ZARR Lyrae stars, thereby giving $M_V(\text{TO})$, to which the bolometric correction is applied.

Figure 10 shows the observed values of $\Delta V(\text{ZAHB} - \text{TO})$ for different $[\text{Fe}/\text{H}]$ values. The data are taken from columns (2) and (6) of Table 3 discussed later. There is no clear trend with metallicity. The mean value for the magnitude difference is 3.54 mag. The accuracy for any given determination is hardly greater than ~ 0.1 mag because of the difficulty of determining (1) the precise level of the turnoff and (2), of less but not negligible importance, the position of the ZAHB. [This latter point is particularly important for 47 Tuc, where the stubby red HB does not extend into the variable star strip, and some decision on the shape of the ZAHB is necessary. It needs only to be pointed out that our adopted $V(\text{ZAHB})$ value for 47 Tuc in Table 1 (col. [5]) is 0.1 mag brighter than adopted by Hesser *et al.* 1987.] We conclude that all of the scatter in Figure 10 could be observational, showing the advantage in using a mean value for $\Delta(\text{TO} - \text{ZAHB})$ rather than any individual value.

C. We can determine the turnoff luminosity directly from the main-sequence fitting procedure discussed in § II.

b) Results

The calculations of ages using method A are detailed in Table 3. The first three columns are the same as in Table 1. The apparent V -magnitude of the zero-age horizontal branch in column (4), corrected for absorption by $3.2E(B - V)$, is adopted from the review by BCF (their Table IV). The observed apparent magnitude of the turnoff (also corrected for absorption) is given in column (5) as read from diagrams plotted from the summary of the main-sequence photometry made by BCF (their Table II). These turnoff magnitudes are the same as listed in column (7) of Table 1. The magnitude differences between columns (4) and (5), listed in column (6), are plotted in Figure 10.

Columns (7)–(12) detail the age calculations that are made by assuming the ZAHB RR luminosities to be $M_V(\text{RR}) = 0.80$, independent of $[\text{Fe}/\text{H}]$, as explained in § V. The distance modulus corrected for absorption is shown in column (8), found by subtracting column (7) from column (4). Subtracting column (8) from column (5) gives the absolute V -magnitude of

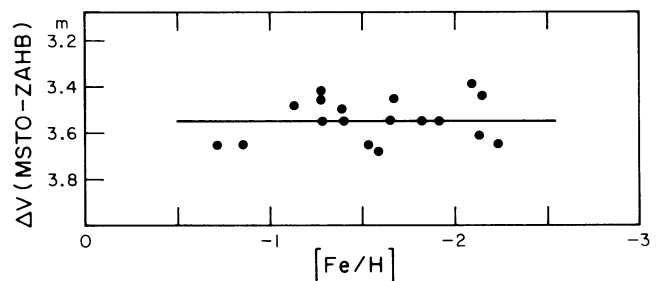


FIG. 10.—Observed difference in apparent V -magnitude between the main sequence and the zero-age horizontal branch as a function of metallicity. Data are from col. (6) of Table 3.

TABLE 3
CLUSTER AGES ASSUMING NO OXYGEN ENHANCEMENT AND USING OBSERVED APPARENT MAGNITUDES OF THE ZAHB AND THE MAIN-SEQUENCE TURNOFF LEVEL WITH ASSUMED $M_V(RR)$ VALUES

Cluster (1)	[Fe/H] (2)	E(B-V) (3)	V_{ZAHB}^0 (4)	$V^0(TO)$ (5)	ΔV (6)	$M_V(TO)$ (7)	$M_V(RR)$ (8)	$(m-M)_0$ (9)	B.C. (10)	M_{bol}^{TO} (11)	Age (12)	$M_V(RR)$ (13)	$(m-M)_0$ (14)	M_{bol}^{TO} (15)	Age (16)	$M_V(RR)$ (17)	$(m-M)_0$ (18)	M_{bol}^{TO} (19)	Age (20)	
																				$M_V(RR) = -0.80$
N104	-0.71	0.04	13.97	17.62	3.65	0.80	13.17	4.45	-0.9	4.36	16.3	1.00	12.97	4.56	19.7	0.99	12.98	4.55	19.5	
N288	-1.40	0.04	15.27	18.82	3.55	0.80	14.47	4.35	-1.1	4.24	18.5	0.86	14.41	4.30	19.6	0.72	14.55	4.16	17.2	
N362	-1.27	0.06	15.24	18.66	3.42	0.80	14.44	4.22	-0.9	4.13	16.0	0.89	14.35	4.22	17.4	0.77	14.47	4.10	15.5	
N2808	-1.37	0.22	15.40	18.40	3.50	0.80	14.60	4.30	-1.1	4.19	17.5	0.87	14.53	4.26	18.7	0.74	14.66	4.13	16.5	
N4590	-2.09	0.07	15.49	18.88	3.39	0.80	14.69	4.19	-1.1	4.08	20.2	0.73	14.76	4.01	18.9	0.45	15.04	3.73	14.5	
N5139	-1.59	0.11	14.17	17.85	3.68	0.80	13.37	4.48	-1.2	4.36	22.1	0.83	13.34	4.39	22.8	0.65	13.52	4.21	19.2	
N5272	-1.66	0.01	15.62	19.07	3.45	0.80	14.82	4.25	-1.1	4.14	18.4	0.81	14.81	4.15	18.6	0.62	15.00	3.96	15.5	
N5904	-1.13	0.03	15.01	18.50	3.49	0.80	14.21	4.29	-1.0	4.19	16.1	0.92	14.09	4.31	18.0	0.83	14.18	4.22	16.5	
N6121	-1.28	0.37	12.17	15.72	3.55	0.80	11.37	4.35	-1.0	4.25	17.9	0.89	11.28	4.34	19.5	0.77	11.40	4.22	17.4	
N6171	-0.85	0.31	14.71	18.36	3.65	0.80	13.91	4.45	-0.9	4.36	17.1	0.97	13.74	4.53	20.1	0.94	13.77	4.50	19.6	
N6205	-1.65	0.02	14.89	18.44	3.55	0.80	14.09	4.35	-1.1	4.24	20.2	0.82	14.07	4.26	20.6	0.63	14.26	4.07	17.2	
N6341	-2.24	0.02	14.99	18.64	3.65	0.80	14.19	4.35	-1.2	4.33	26.9	0.70	14.29	4.23	24.5	0.40	14.59	3.93	18.5	
N6397	-1.91	0.18	12.42	15.97	3.55	0.80	11.62	4.35	-1.2	4.23	21.9	0.77	11.65	4.20	21.3	0.53	11.89	3.96	16.9	
N6752	-1.54	0.04	13.62	17.27	3.65	0.80	12.82	4.45	-1.1	4.34	21.4	0.84	12.78	4.38	22.2	0.67	12.95	4.21	18.9	
N6809	-1.82	0.14	13.90	17.45	3.55	0.80	13.10	4.35	-1.1	4.24	21.4	0.78	13.12	4.22	21.0	0.56	13.34	4.00	17.1	
N7078	-2.15	0.10	15.54	18.98	3.44	0.80	14.74	4.24	-1.2	4.12	21.4	0.72	14.82	4.04	19.9	0.43	15.11	3.75	15.1	
N7099	-2.13	0.04	15.07	18.69	3.62	0.80	14.27	4.42	-1.1	4.31	25.4	0.73	14.34	4.24	23.8	0.44	14.63	3.95	18.1	
Pal 5	-1.27	0.03	17.30	20.75	3.45	0.80	16.50	4.25	-1.0	4.15	16.3	0.89	16.41	4.24	17.7	0.77	16.53	4.12	15.8	

TABLE 4
CLUSTER AGES ASSUMING NO OXYGEN ENHANCEMENT AND USING ASSUMED ABSOLUTE MAGNITUDES OF THE ZAHB TOGETHER WITH $\Delta V = 3.54$ TO THE MAIN-SEQUENCE TURNOFF

Cluster (1)	[Fe/H] (2)	$M_V(RR)$ (3)	$M_V(TO)$ (4)	B.C. (5)	M_{bol}^{TO} (6)	Age (7)	$M_V(RR)$ (8)	M_{bol}^{TO} (9)	Age (10)	$M_V(RR)$ (11)	M_{bol}^{TO} (12)	Age (13)
N104	-0.71	0.80	4.34	-0.9	4.25	14.7	1.00	4.45	17.8	0.99	4.44	17.6
N288	-1.40	0.80	4.34	-1.1	4.23	18.3	0.86	4.29	19.4	0.72	4.15	17.0
N362	-1.27	0.80	4.34	-0.9	4.25	17.9	0.89	4.34	19.4	0.77	4.22	17.4
N2808	-1.37	0.80	4.34	-1.1	4.23	18.1	0.87	4.30	19.4	0.74	4.17	17.1
N4590	-2.09	0.80	4.34	-1.2	4.22	23.3	0.73	4.16	21.8	0.45	3.88	16.7
N5139	-1.59	0.80	4.34	-1.1	4.22	19.4	0.83	4.25	20.0	0.65	4.07	16.8
N5272	-1.66	0.80	4.34	-1.1	4.23	20.1	0.81	4.24	20.2	0.62	4.05	16.9
N5904	-1.13	0.80	4.34	-1.0	4.24	16.9	0.92	4.36	18.9	0.83	4.27	17.3
N6121	-1.28	0.80	4.34	-1.0	4.24	17.8	0.89	4.33	19.3	0.77	4.21	17.3
N6171	-0.85	0.80	4.34	-0.9	4.25	15.5	0.97	4.42	18.1	0.94	4.39	17.6
N6205	-1.65	0.80	4.34	-1.1	4.23	20.0	0.82	4.25	20.4	0.63	4.06	17.0
N6341	-2.24	0.80	4.34	-1.2	4.22	24.3	0.70	4.12	22.1	0.40	3.82	16.6
N6397	-1.91	0.80	4.34	-1.2	4.22	21.7	0.77	4.19	21.1	0.53	3.95	16.8
N6752	-1.54	0.80	4.34	-1.1	4.22	19.2	0.84	4.27	20.0	0.67	4.10	17.0
N6809	-1.82	0.80	4.34	-1.1	4.23	21.2	0.78	4.21	20.8	0.56	3.99	16.9
N7078	-2.15	0.80	4.34	-1.2	4.22	23.5	0.72	4.14	21.8	0.43	3.85	16.6
N7099	-2.13	0.80	4.34	-1.1	4.23	23.6	0.73	4.16	22.1	0.44	3.87	16.8
Pal 5	-1.27	0.80	4.34	-1.0	4.24	17.7	0.89	4.33	19.3	0.77	4.21	17.2

the turnoff in column (9). The bolometric correction in column (10), taken again from the tables used by the Yale group, when applied to column (9) gives the bolometric magnitude of the turnoff in column (11). The age in column (12) (the unit is Gyr) has been calculated from equation (13) by adopting $Y = 0.24$ and $[\text{Fe}/\text{H}]$ from column (2).

Columns (13)–(16) show the same calculation using the RR Lyrae absolute magnitudes listed in column (13), obtained from the BW calibration of equation (9) (§ IV) but referred to the ZAHB by adding 0.1 mag to this equation. Column (14) is column (13) subtracted from column (4). Column (15) is column (14) subtracted from column (5) (with the result not shown), to which the bolometric correction of column (10) is added. The age, again from equation (13), is shown in column (16).

The same calculation in columns (17)–(20) uses the $M_V(\text{RR})$ magnitudes obtained from the pulsation calibration in equation (8) (§ III), again reduced to the ZAHB by adding 0.1 mag. The units for the ages in column (20) are Gyr.

The calculations made using method B above, in which the main-sequence turnoff is determined by adding 3.54 mag to the assumed RR Lyrae absolute magnitudes, are shown in Table 4. Columns (3), (8), and (11) give the adopted RR Lyrae absolute magnitudes based on the three stated assumptions concerning the calibrations of the ZAHB $M_V(\text{RR})$ values that (a) $M_V(\text{RR}) = 0.8$, (b) $M_V(\text{RR}) = 0.19[\text{Fe}/\text{H}] + 1.13$ from equation (9) plus 0.1 mag, and (c) $M_V(\text{RR}) = 0.39[\text{Fe}/\text{H}] + 1.27$ from equation (8) plus 0.1 mag. To these adopted RR Lyrae absolute magnitudes are added 3.54 mag and the main-sequence bolometric correction in column (5) to give the assumed bolometric magnitude of the turnoffs in columns (6), (9), and (12). The ages from equation (13) are listed in columns (7), (10), and (13).

The results from Tables 3 and 4 are shown in Figure 11 using the scale along the left-hand ordinate, which assumes no oxygen enhancement. The ages with $[\text{O}/\text{Fe}]$ enhancement, shown along the right-hand ordinate, are discussed in § VII. The plotted points are the age data for each individual cluster from columns (12), (16), and (20) from Table 3. The scatter here is identical to the scatter in Figure 10, because it is due to the same source. The solid lines are the ages from columns (7), (10), and (13) of Table 4, connected as a continuum. By the method of calculation, there is, of course, no scatter in the Table 4 age values for different metallicities, except for the very small effect due to the slight differences in the bolometric corrections in column (10) of Tables 1 and 3 and column (5) of Table 4.

Figure 11 shows again the well-known fact that whether the ages of the globular clusters vary with metallicity or not depends on the slope of the $M_V(\text{RR})$ –metallicity relation (S82; Buonanno 1986; BCF). If $M_V(\text{RR})$ is independent of metallicity (*top panel*) the age–metallicity dependence is very strong. The top panel of Figure 11 shows an age spread of about 7 Gyr between $[\text{Fe}/\text{H}]$ values of -1 and -2 if $M_V(\text{RR})$ is independent of $[\text{Fe}/\text{H}]$. On the other hand, equation (13) shows that there would be no dependence of age on metallicity if $dM_V(\text{RR})/d[\text{Fe}/\text{H}] = 0.15/0.41 = 0.37$. This value is close to the slope shown in the bottom panel of Figure 11, which is based on the $M_V(\text{RR})$ calibration that uses the period-shift data, combined with the current calculation of double-mode RR Lyrae masses. The average age is 17 Gyr assuming, as throughout this section, no oxygen enhancement as $[\text{Fe}/\text{H}]$ decreases. The systematic age variation in the middle panel, based directly on the BW calibration, is ~ 4 Gyr over the

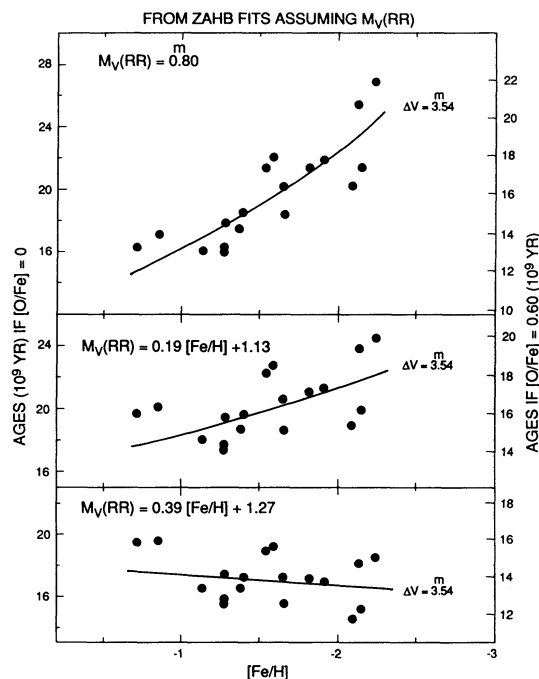


FIG. 11.—Globular cluster ages using three different assumptions for the ZAHB RR Lyrae star absolute magnitudes as functions of metallicity. The age scale on the left is for no oxygen enhancement as $[\text{Fe}/\text{H}]$ decreases. The scale on the right is for an oxygen enhancement of $[\text{O}/\text{Fe}] = +0.6$. The solid lines are from the calculations in Table 4 that use the magnitude difference of 3.54 between the ZAHB and the main-sequence turnoff to determine $M_V(\text{TO})$ of the turnoff.

relevant metallicity range, averaging 20 Gyr at $[\text{Fe}/\text{H}] = -1.6$ and therefore giving a 20% variation.

VII. CLUSTER AGES ASSUMING OXYGEN ENHANCEMENT

Because the metallicity dependence in equation (13) is due primarily to the interior opacity, and because, as said before, the oxygen abundance in any standard mix of the chemical elements is about 250 times the Fe abundance, the effect of O not tracking Fe can be approximated by replacing $[\text{Fe}/\text{H}]$ in equation (13) by $[\text{M}/\text{H}]$ to account for the true opacity. Detailed calculations are, of course, required because the energy generation efficiency is also involved, owing to the competition of the CNO cycle and the PP reaction at the relevant turnoff masses. However, unpublished calculations by Vandenberg (1988a, b) show that the approximation now to be discussed illustrates the principal points. The spectroscopic evidence from field subdwarfs, due primarily to Lambert, Sneden, and their coworkers, and to Bond and Luck (see Sneden 1985 for a review; additional references in Sandage 1988), is strong that oxygen is overabundant relative to Fe in stars where $[\text{Fe}/\text{H}] < -1$. Additional evidence is provided from globular clusters (Gratton 1987) and halo giants (Barbuy 1988). However, Pilachowski (1988) argues that no O enhancement is detected in M92 giants, apparently clouding the issue.²

² However, the value of the $[\text{O}/\text{H}]$ ratio in globular clusters appears still to be open. The O abundance itself is very difficult to measure because of the weakness and the paucity of O lines in the optical spectrum (cf. Fig. 1 of Pilachowski 1988). In a review of globular clusters and age dating, J. W. Truran (1989, private communication) has set out the observational evidence (much from Gratton 1987) that the elements which are expected to be synthesized along with O (Ca, Ti, Mg, etc.), all of which are more easily measured than O, are all overabundant relative to Fe in the globular clusters studied to date.

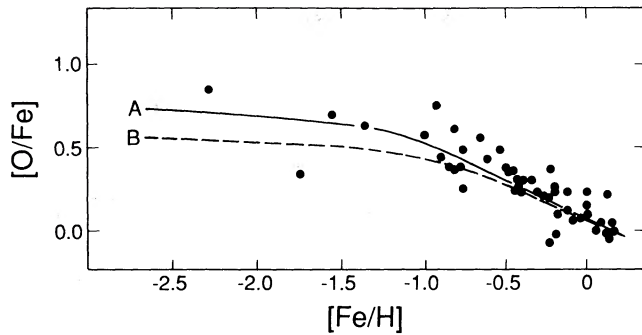


FIG. 12.—Observed oxygen enhancement with decreasing $[\text{Fe}/\text{H}]$ from Sneden (1985). The two lines labeled A and B are from theoretical models of explosive nucleosynthesis of massive stars discussed there.

Figure 12 is from Sneden's review. The two lines are from theoretical models that give the nucleosynthesis abundance yields from exploding massive stars. The filled circles are data for individual stars from the spectroscopic observations. The upper curve (labeled A) is slightly favored from these data.

Over the $[\text{Fe}/\text{H}]$ range relevant for the globular clusters (i.e., $[\text{Fe}/\text{H}] < -1$), the linear approximation to Figure 12 of

$$[\text{O}/\text{Fe}] = c[\text{Fe}/\text{H}] + d \quad (16)$$

is adequate. From the obvious relation that

$$[\text{O}/\text{H}] = [\text{O}/\text{Fe}] + [\text{Fe}/\text{H}] \quad (17)$$

and from the approximation $[\text{M}/\text{H}] = [\text{O}/\text{H}]$, equation (13) becomes

$$\log T = 8.319 + 0.41M_{\text{bol}}(\text{TO}) - 0.15(c+1)[\text{Fe}/\text{H}] - 0.15d. \quad (18)$$

If we assume that $c = 0$ (i.e., no $[\text{Fe}/\text{H}]$ dependence for the $[\text{O}/\text{Fe}]$ enhancement over the relevant $[\text{Fe}/\text{H}]$ range), then the ages decrease by the factor of $0.15d$ in $\log T$. For example, if

$d = +0.6$, and $c = 0$ (note, however, that Gratton's 1987 and Barbuy's 1988 data would rather suggest $d \sim +0.4$ and $c = 0$), then the ages would decrease by $d \log T = 0.09$, or a factor of 1.23.

Sneden's (1985) subdwarf data of Figure 12, however, might be better approximated by a relation which is dependent on $[\text{Fe}/\text{H}]$ according to

$$[\text{O}/\text{Fe}] = -0.14[\text{Fe}/\text{H}] + 0.40, \quad (19)$$

which is about two-thirds of the way between curves A and B in Figure 12 (closer to A). Equation (19) put into equation (18) gives

$$\log T(\text{yrs}) = 8.259 + 0.41M_{\text{bol}}(\text{TO}) - 0.129[\text{Fe}/\text{H}]. \quad (20)$$

The results of using equation (20) to calculate the ages of the program clusters are summarized in Table 5 using the same $M_{\text{bol}}(\text{RR})$ values set out earlier in Tables 3 and 4. Shown in column (3) is the factor by which to multiply the ages in columns (12), (16), and (20) of Table 3 and columns (7), (10), and (13) of Table 4 to obtain the ages via equation (20) for the oxygen enhancement case. These factors for different metallicities are found simply by combining equations (13) and (20). The ages listed in column (7) of Table 5 are for the direct main-sequence fitting data from Table 1. They are the column (12) values from Table 1, multiplied by the factors in column (3) of Table 5.

The results are shown in Figure 13. The slope dependencies in the three panels are slightly different from those in Figure 11 because of the nonzero value of c in equations (16) and (19). In addition, all ages are smaller than those in Figure 11 (*left-hand ordinate*) because of the oxygen enhancement (i.e., all factors in col. [3] of Table 5 are less than unity). The mean age between the middle and the bottom panels of Figure 13 is 15 Gyr, which is larger by $\sim 10\%$ than the ages determined by Vandenberg (1988a, b) from his detailed oxygen-enhanced models. Clearly, firmer conclusions on the effects of oxygen enhancement on age determination will be possible only when unambiguous

TABLE 5
AGES WITH $[\text{O}/\text{Fe}]$ ENHANCEMENT USING FOUR METHODS TO OBTAIN $M_{\text{bol}}^{\text{TO}}$

Cluster (1)	$[\text{Fe}/\text{H}]$ (2)	Factor (3)	Age (4)	$M_v = +0.8$			Age (7)
				$.19[\text{Fe}/\text{H}] + 1.13$	$.39[\text{Fe}/\text{H}] + 1.27$	Direct MS	
N104	-0.71	0.842	13.7			16.4	15.4
N288	-1.40	0.814	15.0			14.0	15.9
N362	-1.27	0.819	13.1			12.7	15.5
N2808	-1.37	0.815	14.3			13.4	15.1
N4590	-2.09	0.787	15.9			11.4	12.6
N5139	-1.59	0.806	17.8			15.5	17.0
N5272	-1.66	0.804	14.8			12.5	14.9
N5904	-1.13	0.825	13.3			13.6	14.6
N6121	-1.28	0.819	14.7			14.2	16.6
N6171	-0.85	0.836	14.3			16.4	(20.9)
N6205	-1.65	0.804	16.2			13.8	18.2
N6341	-2.24	0.782	21.0			14.5	19.0
N6397	-1.91	0.794	17.4			13.4	13.8
N6752	-1.54	0.808	17.3			15.3	16.5
N6809	-1.82	0.798	17.1			13.6	13.7
N7078	-2.15	0.785	16.8			11.8	13.8
N7099	-2.13	0.786	20.0			14.2	14.8
Pal 5	-1.27	0.819	13.3			12.9	13.8
							15.4 \pm 1.7

observational evidence and O-enhanced isochrones become available.³

VIII. CLUSTER AGES DETERMINED FROM THE DIRECT MAIN-SEQUENCE FITS

No assumptions about RR Lyrae star absolute magnitudes are needed to determine the ages using the M_{bol} values of the turnoff determined directly from the main-sequence fits. These bolometric turnoff magnitudes, listed in column (11) of Table 1, when put into equations (13) and (20) give the ages set out in columns (12) and (7) of Tables 1 and 5, respectively.

The results are shown in Figure 14, where the ages from equation (13) are marked on the left-hand ordinate; those on the right are for $c = 0$ and $d = 0.6$ in equation (16), producing a factor of 1.23 between the cases of no [O/Fe] enhancement and [O/Fe] enhancement. The mean ages derived from these data are 19.1 and 15.5 Gyr, respectively, nearly identical to the mean of the middle and bottom panels of Figures 11 and 13. Furthermore, there is no evidence in Figure 14 for a variation of age with [Fe/H] from this main-sequence fitting method. This result, of course, is obvious because the slope of the main-sequence fitting method for $M_V(\text{RR})$ in equations (4) and (5) is close to the 0.37 required by equation (13) for no [Fe/H] dependence for the ages, provided, of course, that the $\Delta V(\text{TO} - \text{ZAHB})$ magnitude difference is as independent of [Fe/H] as is indicated by the available data (Fig. 10).

A different representation of Figure 14 is shown in Figure 15, where the turnoff magnitudes from column (11) of Table 1 are plotted against metallicity. Lines of constant age from equation (13) are labeled along the top. The corresponding ages, reduced by a factor of 1.23 for an [O/Fe] enhancement of 0.6, are shown at the bottom of each constant-age line. The least-squares line for the $M_{\text{bol}}(\text{TO})$ versus [Fe/H] regression is

$$M_{\text{bol}}(\text{TO}) = 0.34[\text{Fe}/\text{H}] + 4.739, \quad (21)$$

where the uncertain point of NGC 6171 is omitted. The correlation coefficient is $r = 0.78$. The slope of equation (21) of 0.34 is close to the 0.37 needed according to equation (13) to give no age dependence of the globular cluster system on metallicity. On the other hand, equation (9) from the BW method gives the much more shallow slope of 0.19, requiring a 20% variation of age with [Fe/H]. At the moment there is no understanding of how to reconcile these contrary results, or how to decide which is the more reliable solution (cf. the Appendix).

IX. SUMMARY

Evidence has been presented that many calibrations of the absolute luminosities of zero-age horizontal-branch RR Lyrae stars show a dependence on metallicity. These calibrations include (1) the period-density pulsation equation applied to both field and cluster variables, combined with the masses

³ It is to be noted that we should not apply a correction to the adopted RR Lyrae absolute magnitudes for the difference between [Fe/H] and [O/H] in this oxygen enhancement case. The calibrations of $M_V(\text{RR})$ in this paper and in the one which precedes it (S90b) give $M_V(\text{RR})$ directly by any of the three methods used (pulsation, main-sequence fitting, and Baade-Wesselink), independent of whatever value is taken for the chemical composition of the clusters or of the field variable that are involved. The correlation with chemical composition is, then, with the actual values of the compositions of these calibrating objects. Hence, throughout this series we should have written the absolute magnitude equations as $M(\text{RR}) = a[\text{M}/\text{H}] + b$ rather than $M(\text{RR}) = a[\text{Fe}/\text{H}] + b$. We are indebted to A. Sweigart for raising this issue.

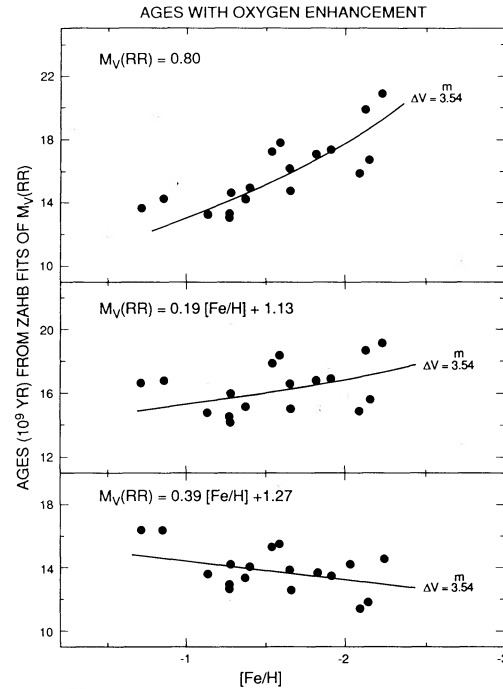


FIG. 13.—Same as Fig. 11, but using an [O/Fe] enhancement of $[\text{O}/\text{Fe}] = -0.14[\text{Fe}/\text{H}] + 0.40$ from eq. (19).

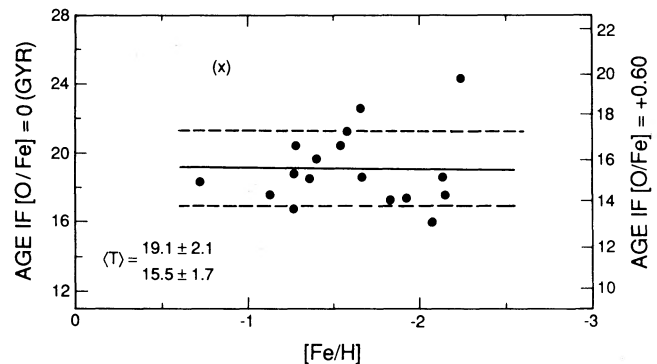


FIG. 14.—Globular cluster ages as a function of metallicity determined using $M_{\text{bol}}(\text{TO})$ values that have been found directly from main-sequence fits, as listed in col. (11) of Table 1. The ages with and without oxygen enhancement are calculated from eqs. (13) and (20).

determined from the double-mode variables; (2) the Baade-Wesselink method applied to field variables; (3) main-sequence fitting of $C-M$ diagrams to obtain distances to clusters that contain RR Lyrae variables; and (4) the existing theory (SRT) of the position of the ZAHB as a function of metallicity.

The various RR Lyrae absolute magnitude calibrations have been used in several ways to determine the absolute bolometric luminosities of cluster turnoff positions. The resulting calculated cluster ages either (1) depend strongly on metallicity if $M_V(\text{RR})$ is not a function of [Fe/H], (2) are independent of metallicity if $dM_V(\text{RR})/d[\text{Fe}/\text{H}] = 0.37$, or (3) have an intermediate dependence if the slope of the RR Lyrae luminosity-metallicity dependence is between zero and 0.37. For the case using the $M_V(\text{RR})$ calibration by the Baade-Wesselink method where $dM_V(\text{RR})/d[\text{Fe}/\text{H}] = 0.19$, the variation of cluster age

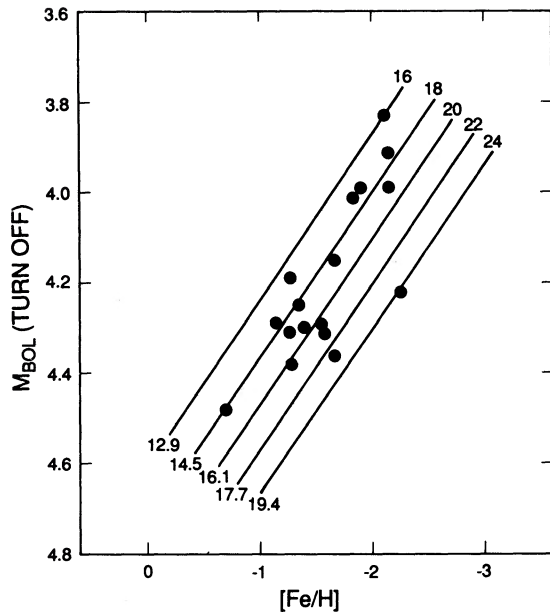


FIG. 15.—Correlation of the metallicity and the turnoff luminosity, $M_{\text{bol}}(\text{TO})$, that has been found from the main-sequence fits from Figs. 3 and 4 as listed in cols. (2) and (11) of Table 1. Lines of constant age from eq. (13) are shown as marked on the top for no oxygen enhancement. The ages marked on the bottom are for an oxygen enhancement of $[\text{O}/\text{Fe}] = +0.6$, giving ages reduced by a factor of 1.23, as listed in col. (7) of Table 5.

with metallicity is $\sim 20\%$ over the observed metallicity range, with the most metal-poor clusters being oldest.

The absolute ages calculated from the original Yale (Ciardullo and Demarque 1977) isochrones are in good agreement ($\sim 7\%$) with the independent isochrones of Vandenberg and Bell (1985). Without oxygen enhancement, the mean age of the globular cluster system for the case where $dM_V(\text{RR})/d[\text{Fe}/\text{H}] = 0.37$ is 17 Gyr using the RR Lyrae calibration of equation (8) via the period-shift analysis when it is reduced to the ZAHB. This calibration then becomes $M_V(\text{RR}) = 0.39[\text{Fe}/\text{H}] + 1.27$. The slightly fainter calibration from the Baade-Wesselink method from equation (9), applied to field stars and reduced to the ZAHB, becoming $M_V(\text{RR}) = 0.19[\text{Fe}/\text{H}] + 1.13$, gives absolute ages that range between 18 and 22 Gyr for $[\text{Fe}/\text{H}]$ values between -0.8 and -2.2 .

These ages are all decreased by a factor of 1.23 if there is an oxygen enhancement of $[\text{O}/\text{Fe}] = +0.6$ for $[\text{Fe}/\text{H}] < -0.8$. If, instead of a fixed value for this offset, the enhancement were to have a slope with $[\text{Fe}/\text{H}]$ as in curve A of Figure 12, the constant-age case (i.e., independent of metallicity) would occur for an RR Lyrae calibration which has a smaller slope than

$dM_V(\text{RR})/d[\text{Fe}/\text{H}] = 0.37$ (cf. eq. [20], where the constant-age slope would be 0.31; the larger the value of c in eq. [16], the smaller the slope must be for the constant-age case).

The chief unsolved problem at the moment is an explanation of why the various RR Lyrae absolute magnitude calibrations (cf. Fig. 8) give such different slope dependencies on metallicities. Both the pulsation period-shift method and the main-sequence fitting methods give steeper slopes than the BW method by larger factors than their internal errors (compare Figs. 5 and 7). This shows that there are systematic errors in at least one of the methods, but we cannot at the moment determine which, if not both. The main-sequence fitting methods suffer from (1) the extreme sensitivity of the results to the assumptions of the positions of the fiducial main sequences for different $[\text{Fe}/\text{H}]$ values (Figs. 3 and 4), (2) remaining photometric errors in the main-sequence CCD photometry and reddening corrections, and (3) use of different fitting procedures which weight different parts of the C - M diagram differently. Very slight differences in the positions of the adopted sequences in Figure 4 could bring agreement between the main-sequence fitting method and the BW method, as regards the slope of the metallicity dependence. However, one is then left with the steep slope of ~ 0.4 from the period-shift analysis (S90b) of the RR Lyrae stars themselves (or its equivalent analysis via the $L/M^{0.81}$ ratio). This method is independent of the main-sequence fittings, depending as it does only on the pulsation properties of the stars. But the principal uncertainty here is which value of the mass should be used to eliminate the mass term from the $L/M^{0.81}$ ratio (Lee, DeDemarque, and Zinn 1990; S90b), which itself is strongly affected by the assumptions made in the double-mode pulsator model calculations.

Finally, ages of the globular clusters can be determined independently of the calibration of RR Lyrae absolute luminosities entirely if we rely on the main-sequence fits to determine $M_{\text{bol}}(\text{TO})$ directly. The result from § VIII is that the mean age is either 15 or 19 Gyr (depending on the existence or non-existence of oxygen enhancement), with no appreciable dependence of the ages on metallicity (Figs. 14 and 15).

We wish to thank F. Fusi Pecci for helpful comments and suggestions during the preparation of this paper and for additional suggestions in his role as the referee of the paper as it was originally submitted. It is also a pleasure to thank A. Sweigart and D. Vandenberg for their careful reading of an early draft and for their suggestions for improvement. One of us (A. S.) again wishes to thank Y.-W. Lee, P. Demarque, and R. Zinn for a detailed conversation concerning many aspects of the RR Lyrae problem. It is a pleasure to thank Janet Krupsaw of The Johns Hopkins University for the preparation of the manuscript.

APPENDIX

$M_V(\text{RR})$ FROM FITS TO THE FAMILY OF FIDUCIAL MAIN SEQUENCES DEFINED IN THE REVISED (1987) YALE ISOCHRONE TABLES

In view of the difference in the metallicity dependence of $M_V(\text{RR})$ that has been derived in the text between main-sequence fits to the Vandenberg and Bell (1985) isochrones and the Baade-Wesselink method, we inquire here whether main-sequence fits of the same data we have used (i.e., those of BCF) to the revised Yale isochrones (Green, Demarque, and King 1987) can give the smaller slope of $dM_V(\text{RR})/d[\text{Fe}/\text{H}] = 0.2$. This shallower slope is not only that given by the current BW data but is also the predicted slope in the LDZ model concerning period shifts due to post-ZAHB evolution. On the other hand, an analysis of the period-shift data

TABLE 6
YALE (1987) FIDUCIAL ZAMS FOR DIFFERENT $[\text{Fe}/\text{H}]^a$

$(B-V)/[\text{Fe}/\text{H}]$ (1)	M_V					
	0 (2)	-0.23 (3)	-0.63 (4)	-1.23 (5)	-1.62 (6)	-2.23 (7)
0.35.....	3.16	3.44	3.86	4.26	4.45	4.60
0.40.....	3.43	3.72	4.14	4.60	4.77	4.96
0.45.....	3.74	4.04	4.46	4.95	5.12	5.32
0.50.....	4.01	4.33	4.76	5.31	5.47	5.68
0.55.....	4.32	4.64	5.17	5.67	5.83	6.02
0.60.....	4.68	5.01	5.55	6.01	6.18	6.32
0.65.....	5.03	5.40	5.89	6.30	6.48	6.61
0.70.....	5.37	5.73	6.20	6.59	6.75	6.88
0.75.....	5.70	6.04	6.49	6.81
0.80.....	6.00	6.39	6.76
0.85.....	6.31	6.64	7.00
0.90.....	6.62	6.87

^a Shapes are interpolated from the Yale 1987 tables for $Y = 0.25$. The zero point in M_V is from trigonometric parallax stars of high weight with $\langle[\text{Fe}/\text{H}]\rangle = 0$.

themselves (S90b) has continued to give a steep slope dependence of 0.39, similar to that found from the main-sequence fits to the Vandenberg and Bell isochrones. In view of the result by Green (1988) that her main-sequence fits of globular cluster main-sequence data to the Yale isochrones give the shallower slope of 0.2, we set out in this appendix an independent analysis of fits of the BCF data to the Yale isochrones.

Our procedures to fit the Yale isochrones are as follows:

1. The zero-age main sequences from the Yale tables for the helium abundances $Y = 0.2$ and 0.3 and for $[\text{Fe}/\text{H}]$ values of 0 , -0.23 , -0.63 , -1.23 , -1.62 , and -2.2 have been interpolated to a helium abundance of $Y = 0.25$.

2. The M_V zero point of this family of fiducial ZAMS positions has been set by forcing agreement with Figure 1 of the text, defined by the trigonometric parallax stars of high weight with solar abundance (in the mean). Comparison of the shape of the Yale $[\text{Fe}/\text{H}] = 0$ fiducial sequence from step 1 with equation (2) of the text shows a systematic deviation of the Yale ZAMS from the line in Figure 1 (which is eq. [2] that agrees with the parallax data for real stars) for colors between $B - V = 0.5$ and 0.6 , and again for $B - V$ redder than 0.7 . We have made the zero-point fit of Figure 1 to the Yale fiducial $[\text{Fe}/\text{H}] = 0$ main sequence at $B - V = 0.4$ and 0.65 , where the two curves intersect. We suspect that the slight difference in shape between equation (2) and the Yale ZAMS for $[\text{Fe}/\text{H}] = 0$ is due to the color corrections applied by Green (1988, Fig. 1b) in her color-temperature transformation procedures. The resulting family of fiducial ZAMS positions for various $[\text{Fe}/\text{H}]$ values is set out in Table 6.

3. The main-sequence photometric data that we have used in the main part of the paper (from BCF) were fitted to the family of curves in Table 6, after correcting for the adopted reddening (Tables 1, 3, 4, and 5), interpolated to the adopted $[\text{Fe}/\text{H}]$ values. The resulting distance moduli are listed in column (4) of Table 7. These, applied to the column (5) values of the observed ZAHB

TABLE 7
MAIN-SEQUENCE FITS TO YALE (1987) ZAMS MODELS TO DETERMINE $M_V(\text{RR})$ AND $M_{\text{bol}}(\text{TO})$

Cluster (1)	$[\text{Fe}/\text{H}]$ (2)	$E(B-V)$ (3)	$(m-M)_o$ (4)	V_{HB}^o (5)	M_{RR} (6)	$V_o(\text{TO})$ (7)	BC (8)	$M_{\text{bol}}^{\text{TO}}$ (9)
N104	-0.71	0.04	12.95	13.97	1.02	17.62	0.09	4.58
N288	-1.40	0.04	14.47	15.27	0.80	18.82	0.11	4.24
N362	-1.27	0.06	14.29	15.24	0.95	18.66	0.09	4.28
N2808	-1.37	0.22	14.52	15.40	0.88	18.90	0.11	4.27
N4590	-2.09	0.07	15.16	15.49	0.33:	18.88	0.11	3.61
N5139	-1.59	0.11	13.41	14.17	0.76	17.85	0.12	4.32
N5272	-1.66	0.01	14.77	15.62	0.85	19.07	0.11	4.19
N5904	-1.13	0.03	14.03	15.01	0.98	18.50	0.10	4.37
N6121	-1.28	0.37	11.29	12.17	0.88	15.72	0.10	4.33
N6171	-0.85	0.31	13.46	14.71	1.25	18.36	0.09	4.81
N6205	-1.65	0.02	14.18	14.89	0.71	18.44	0.11	4.15
N6341	-2.24	0.02	14.30	14.99	0.69	18.64	0.12	4.22
N6397	-1.91	0.18	11.93	12.42	0.49	15.97	0.12	3.92
N6752	-1.54	0.04	13.14	13.62	0.48	17.27	0.11	4.02
N6809	-1.82	0.14	13.54	13.90	0.38	17.45	0.11	3.80
N7078	-2.15	0.10	14.98	15.54	0.56	18.98	0.12	3.88
N7099	-2.13	0.04	14.57	15.07	0.50	18.69	0.11	4.01
Pal 5	-1.27	0.03	16.45	17.30	0.85	20.75	0.10	4.20

apparent magnitudes, corrected for absorption, give the $M_V(\text{RR})$ absolute magnitudes which we seek, listed in column (6). The bolometric magnitudes of the turnoffs in column (9) are determined by applying the column (4) moduli to the observed turnoff apparent magnitudes, corrected for absorption in column (7), to which the bolometric corrections listed in column (8) are applied.

The least-squares solution for the correlation of $M_V(\text{RR})$ in column (6) with the metallicity in column (2), taking $M_V(\text{RR})$ as the independent variable, gives

$$M_V(\text{RR}) = 0.37[\text{Fe}/\text{H}] + 1.32, \quad (\text{A1})$$

which is nearly identical with equation (1) of the text. Therefore, we have not been able to reproduce the shallow slope obtained by Green (1988, § 4.2) of $dM(\text{RR})/d[\text{Fe}/\text{H}] = 0.2$ using the above procedure for fitting the BCF photometric data to the revised Yale isochrones, and therefore we cannot confirm the age spread among the globular clusters of different metallicities deduced from such a shallow slope.

A different demonstration of the same conclusion is provided by the least-squares solution for the correlation of the turnoff magnitude itself, $M_{\text{bol}}(\text{TO})$, in column (9) of Table 7 with $[\text{Fe}/\text{H}]$. The solution, taking $M_{\text{bol}}(\text{TO})$ as the independent variable, is

$$M_{\text{bol}}(\text{TO}) = 0.44[\text{Fe}/\text{H}] + 0.44, \quad (\text{A2})$$

excluding NGC 6171. This is even steeper than we obtained in the main text (eq. [21]), were we found a slope of 0.34. Recall that a slope of 0.37 (cf. eq. [13]) is the null slope for no variation of age with $[\text{Fe}/\text{H}]$. A steeper slope than this requires that more metal-poor clusters are younger than the more metal-rich clusters, which would seem to be unphysical.

Of course, the shallow slope of 0.2 from the BW method remains a principal disagreement. We could well argue that, in fact, this is the correct slope (which is also required by the model of LDZ that has a number of attractive features), and that systematic effects due to incorrect assumptions have produced the steeper slopes in the pulsation and the main-sequence methods. In the pulsation method that gives a slope of ~ 0.4 , it has been assumed that the RR Lyrae mass dependence on $[\text{Fe}/\text{H}]$ is given correctly by the double-mode calculations fitted to the observations in M15, M3, and IC 4499. As discussed by LDZ and by Sandage (1990b), the double-mode theory has not yet been worked out for different $[\text{Fe}/\text{H}]$ values; a high sensitivity of calculated mass to changes in $[\text{Fe}/\text{H}]$ could reduce the derived mass difference between the high- and low-metallicity clusters (i.e., M3 and IC 4499 versus M15), reducing the derived slope of $dM_V(\text{RR})/d[\text{Fe}/\text{H}]$. In the main-sequence fitting method, the result depends sensitively on the positions of the various fiducial main sequences for different metallicities.

In the text, and above in this appendix, we have kept the helium abundance constant, and further have neglected any effect of $[\text{O}/\text{Fe}]$ enhancement on the main-sequence positions for $[\text{Fe}/\text{H}]$ that are in the range from 0 to -1 . When a grid of fiducial main-sequence positions for various $[\text{O}/\text{Fe}]$ abundances becomes available, a self-consistent set of fiducials to which to fit the photometric data should be used in which the Y abundance is changed progressively from, say, $Y = 0.27$ for the $[\text{Fe}/\text{H}] = 0$ case (see Vandenberg and Poll 1989 for a justification that $Y = 0.27$ is the correct value to use for ZAMS stars with $[\text{Fe}/\text{H}] = 0$) to $Y = 0.23$ for $[\text{Fe}/\text{H}] = -2$ (assuming this to be the initial value for Population II stars), and with the $[\text{O}/\text{Fe}]$ progressively changed according to some version of Figure 12. Such a self-consistent grid might then give a shallow slope to the $M_V(\text{RR})$ metallicity correlation, reconciling all three methods of calibrating $M_V(\text{RR})$. The necessary models for fiducial main-sequence positions are not yet available, nor have the necessary double-mode mass calculations for different metallicities been made for the problem of the pulsation luminosities. Therefore, the prospects of reconciling the results of the three methods of calibrating the RR Lyrae luminosities clearly have not yet been exhausted.

REFERENCES

- Barbuy, B. 1988, *Astr. Ap.*, **191**, 121.
 Barnes, T. G., and Hawley, S. L. 1986, *Ap. J. (Letters)*, **307**, L9.
 Buonanno, R. 1986, *Mem. Soc. Astr. Italiana*, **57**, 333.
 Buonanno, R., Corsi, C. E., and Fusi Pecci, F. 1988, *Astr. Ap.*, **216**, 80 (BCF).
 Cacciari, C., Clementini, G., and Buser, R. 1988, *Astr. Ap.*, **209**, 154.
 Cacciari, C., Clementini, G., Prévot, L., and Buser, R. 1988, *Astr. Ap.*, **209**, 141.
 Cameron, L. M. 1985, *Astr. Ap.*, **146**, 59.
 Ciardullo, R. B., and Demarque, P. 1977, *Trans. Yale Univ. Obs.*, Vol. **33** (CD).
 Eggen, O. J. 1987, *A.J.*, **93**, 393.
 Eggen, O. J., and Sandage, A. 1962, *Ap. J.*, **136**, 735.
 Gautschi, A. 1987, *Vistas Astr.*, **30**, 197.
 Gratton, R. 1987, *Astr. Ap.*, **177**, 177.
 Green, E. M. 1988, in *Calibration of Stellar Ages*, ed. A. G. D. Philip (*Van Vleck Obs. Contr.*, No. 7; Schenectady: Davis), p. 81.
 Green, E. M., Demarque, P., and King, C. R. 1987, *The Revised Yale Isochrones and Luminosity Functions* (New Haven: Yale University Observatory).
 Hawley, S. L., Jeffreys, W. H., Barnes, T. G., and Lai, W. 1986, *Ap. J.*, **302**, 626.
 Hesser, J. E., Harris, W. E., Vandenberg, A. A., Allwright, J. W. B., Shott, P., and Stetson, P. B. 1987, *Pub. A.S.P.*, **87**, 739.
 Hodge, P. M., and Wallerstein, G. 1966, *Pub. A.S.P.*, **78**, 411.
 Iben, I., and Rood, R. T. 1970, *Ap. J.*, **159**, 605.
 Jameson, R. F., Fernley, J. A., and Longmore, A. J. 1987, *M.N.R.A.S.*, in press.
 Jenkins, L. F. 1952, *General Catalog of Trigonometric Stellar Parallaxes* (New Haven: Yale University Observatory).
 Jones, R. V., Carney, B. W., and Latham, D. W. 1988, *Ap. J.*, **332**, 206.
 Lee, Y.-W., Demarque, P., and Zinn, R. 1990, *Ap. J.*, **350**, 155 (LDZ).
 Liu, T., and Janes, K. A. 1988, in *Calibration of Stellar Ages*, ed. A. G. D. Philip (*Van Vleck Obs. Contr.*, No. 7; Schenectady: Davis), p. 141.
 Lub, J. 1987, in *Stellar Pulsation*, ed. A. N. Cox, W. M. Sparks, and S. G. Starrfield (Lecture Notes in Physics, No. 274; Berlin: Springer-Verlag), p. 218.
 Lutz, T. E., and Kelker, D. H., 1973, *Pub. A.S.P.*, **85**, 573.
 Noble, R., and Dickens, R. J. 1988, in *New Ideas in Astronomy*, ed. F. Bertola, J. W. Sulentic, and B. F. Madore (Cambridge: Cambridge University Press), p. 59.
 Pilachowski, C. 1988, *Ap. J. (Letters)*, **326**, L57.
 Sandage, A. 1958, in *Stellar Populations*, ed. D. O'Connell (*Ric. Astr.*, **5**, 41).
 ———. 1970, *Ap. J.*, **162**, 841.
 ———. 1982, *Ap. J.*, **252**, 553 (S82).
 ———. 1988, *Ap. J.*, **331**, 583.
 ———. 1990a, *Ap. J.*, **350**, 603 (S90a).
 ———. 1990b, *Ap. J.*, **350**, 631 (S90b).
 Sandage, A., and Eggen, O. J. 1959, *M.N.R.A.S.*, **119**, 278.
 Sandage, A., Katem, B. N., and Sandage, M. 1981, *Ap. J. Suppl.*, **46**, 41.
 Sandage, A., and Schwarzschild, M. 1952, *Ap. J.*, **116**, 463.
 Schönberg, M., and Chandrasekhar, S. 1942, *Ap. J.*, **96**, 161.
 Schwarzschild, M. 1958, in *Stellar Populations*, ed. D. J. K. O'Connell (*Ric. Astr.*, **5**, 207).
 Seares, F. H. 1944, *Ap. J.*, **100**, 255.
 Simoda, J., and Iben, I. 1968, *Ap. J.*, **152**, 509.
 ———. 1970, *Ap. J. Suppl.*, **22**, 81.
 Sneden, C. 1985, in *Production and Distribution of CNO Elements*, ed. I. J. Danziger, F. Matteucci, and K. Kjar (Garching: ESO), p. 1.
 Sweigart, A. V., Renzini, A., and Tornambè, A. 1987, *Ap. J.*, **312**, 762 (SRT).
 van Altena, W. F., Lee, J. T., Hansen, R. B., and Lutz, T. E. 1988, in *Calibration of Stellar Ages*, ed. A. G. D. Philip (*Van Vleck Obs. Contr.*, No. 7; Schenectady: Davis), p. 175.

- VandenBerg, D. A. 1983, *Ap. J. Suppl.*, **51**, 29.
———. 1988a, in *Calibration of Stellar Ages*, ed. A. G. D. Philip (*Van Vleck Obs. Contr.*, No. 7; Schenectady: Davis), p. 117.
———. 1988b, in *The Extragalactic Distance Scale*, ed. S. van den Bergh (ASP Conf. Series).
- VandenBerg, D. A., and Bell, R. A. 1985, *Ap. J. Suppl.*, **58**, 561 (VB).
VandenBerg, D. A., and Bridges, T. J. 1984, *Ap. J.*, **278**, 679.
VandenBerg, D. A., and Poll, H. E. 1989, *A.J.*, **98**, 1451.
Wallerstein, G., and Carlson, M. 1960, *Ap. J.*, **132**, 276.
Wallerstein, G., and Hodge, P. 1967, *Ap. J.*, **150**, 951.

CARLA CACCIARI: Osservatorio Astronomico di Bologna, Via Zamboni 33, 40126 Bologna, Italy

ALLAN SANDAGE: The Observatories of the Carnegie Institution of Washington, 813 Santa Barbara Street, Pasadena, CA 91101-1292